INTERNATIONAL ATOMIC ENERGY AGENCY
UNITED NATIONS EDUCATIONAL, SCIENTIFIC AND CULTURAL ORGANIZATION
INTERNATIONAL CENTRE FOR THEORETICAL PHYSICS
I.C.T.P., P.O. BOX 586, 34100 TRIESTE, ITALY, CABLE: CENTRATOM TRIESTE

UNITED NATIONS INDUSTRIAL DEVELOPMENT ORGANIZATION

INTERNATIONAL CENTRE FOR SCIENCE AND HIGH TECHNOLOGY
c/o INTERNATIONAL CENTRE FOR THEORETICAL PHYSICS 34100 TRIESTE (ITALY) VIA GRIGNANO, 9 (ADRIATICO PALACE) P.O BOX 586 TELEPHONE 040-224572 TELEFAX 040-224575 TELEX 460449 APH I

SMR. 628 - 5

Research Workshop in Condensed Matter,
Atomic and Molecular Physics
(22 June - 11 September 1992)

- -

Working Party on
"NOISES IN MESOSCOPIC SYSTEMS"
(27 July - 7 August 1992)

- -

"Charging Effects in Ultrasmall Tunnel Junctions"

M. JONSON
Chalmers University of Technology
Department of Applied Physics
Gothenburg S-41296
SWEDEN

These are preliminary lecture notes, intended only for distribution to participants.

CHARGING EFFECTS IN ULTRASMALL TUNNEL JUNCTIONS

—

CROSSROADS BETWEEN FUNDAMENTAL PHYSICS AND TECHNOLOGY

Jats Jonson, Göteborgs universitet

Collaborators in published work:		Cooperation in Göteborg also with:
K. Flensberg	ORNL, Nordita	T. Claeson
L. Glazman	U. Minnesota	P. Delsing
S.M. Girvin	Indiana U	D. Haviland
D. Penn	NIST	M. Gisselfält
M. Stiles	NIST	R. Shekhter
M.J.	GU	....

Original work mainly on effects of the electromagnetic environment:

Phys. Rev. Lett. **64**, 3183 (1990)

Z. Phys. B**85**, 395 (1991)

Phys. Rev. B**43**, 7586 (1991)

~~Phys. Rev. B (submitted)~~

Physica Scripta '92 (in press)

—

Some recent and forthcoming reviews:

D.V. Averin and K.K. Likharev, in *Mesoscopic Phenomena in Solids*, eds. B.L. Altshuler, P.A. Lee and R.A. Webb, Elsevier, Amsterdam, 1991

G. Schön and A.D. Zaikin, Physics Rep. **198**, 238 (1990)

Z. Phys. B**85**(Dec. 1991) proceedings volume, Les Houches winter school

K.K. Likharev and T. Claeson, Scientific American (to appear)

OUTLINE

A. Normal tunnel junctions

- The "Coulomb blockade" – a brief history
- Hints of applications: "single electronics" (transistors, electrometer)
- Single junction case: Effects of the electrodynamic environment (original work)
- Electron "turnstiles" and - "pumps": A new current standard?

B. Superconducting tunnel junctions

- Coulomb blockade of Cooper pair tunneling
- "Bloch oscillations": time-ordered tunneling of Cooper pairs

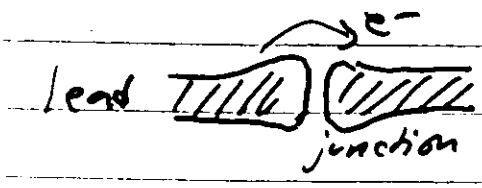

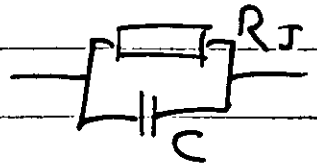

BASICS!

Energy cost of tunneling: $e^2/2C$ So need $V > V_{th} = e/2C$ for net gain.

" gain in " : eV For $V < V_{th}$ there is a Coulomb Blockade of tunneling

$k_B T < e^2/2C$ avoid thermal smearing If junction area $(0.1\ \mu m)^2$ need $T < 0.4$ K for Al/AlO/Al

$h/R_J C < e^2/2C$ avoid quantum smearing (fr. uncertainty principle) $R_J > R_H = h/e^2 \approx 25\ k\Omega$

SOME THEORETICAL PREDICTIONS ≈ 1985 - 86

(Averin, Likharev; Ben-Jacob, Gefen; ...)

a) **Coulomb blockade of tunneling**

Blockade at small V, offset at large V

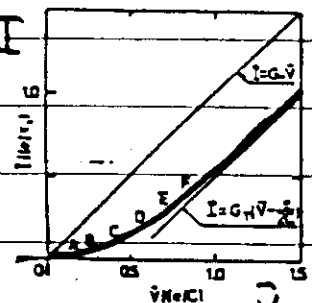

b) **Current biased junction shows voltage fluctuations of $v = I_{bias}/e$.**

Shows up as "inverse Shapiro steps" in presence of microwave radiation.

~~A possible standard for the Amp~~ ?
(Josephson effect now gives standard for Volt)

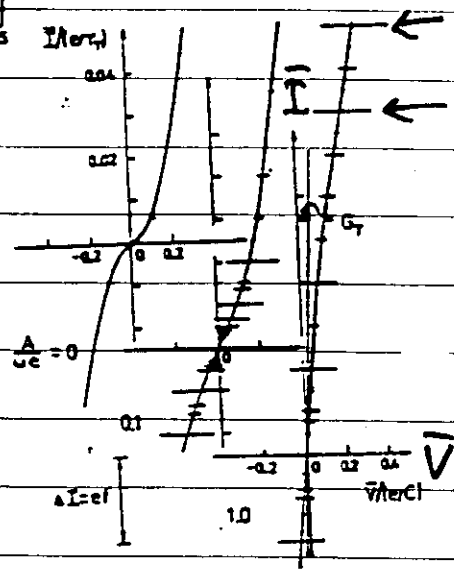

c) **SET (Single Electron Tunn.) Transistors.**

Double junction systems: Tunneling affected by amount of charge on central electrode. Control by gate and get transistor.

Possibly high packing density, smaller size means larger charging effect. 2D and 3D?.

Proiblems: ~~Impedance matching~~?

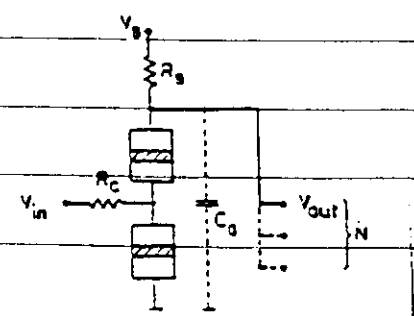

a)-c) for both normal and superconducting jn's

Early observation of Coulomb blockade

I. Giaever and H.R. Zeller, Phys. Rev. Lett. 20, 1504 (1968)

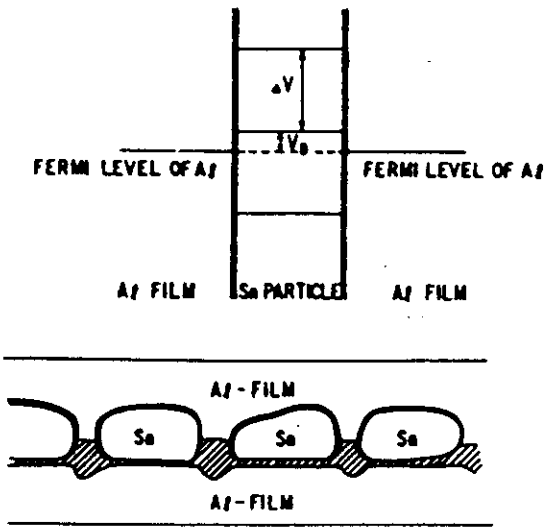

FIG. 1. Model and level scheme of Sn particles in a tunnel junction. V_D is the energy in eV of the last filled state at $T = 0$ of the Sn particle, with respect to the Fermi energy of Al. $\Delta V = e/C$ is the voltage change of the particle caused by addition of one electron. In equilibrium $-e/2C \geq V_D \geq e/2C$ holds.

SUPPRESSION OF CONDUCTANCE
(INCREASE OF RESISTANCE)

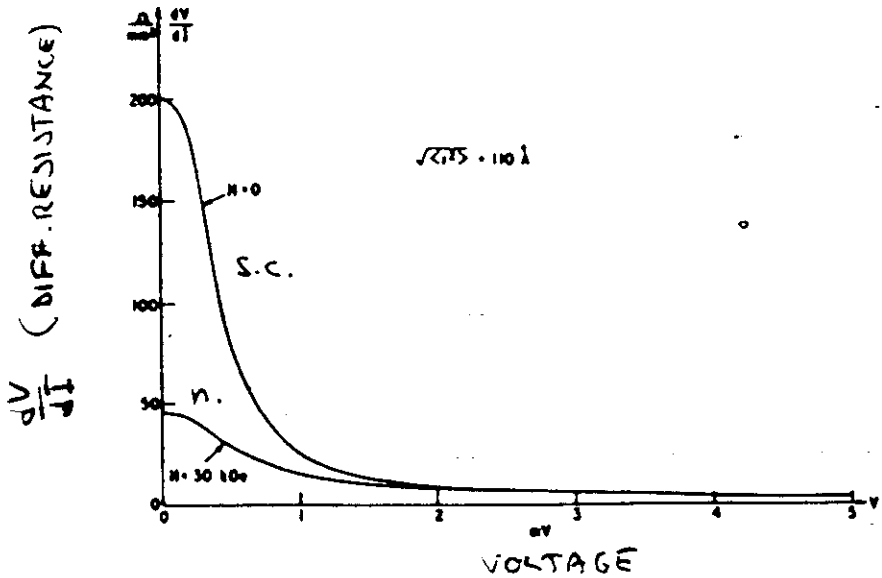

FIG. 2. Dynamical resistance-versus-voltage characteristics for normal and superconducting particles at $T = 1.6°K$. For particles with $r = 110$ Å, H_c is 13 kOe so that all particles are normal at $H = 30$ kOe.

"PROBLEM": TUNNELING THROUGH MANY Sn PARTICLES.
WHAT IS "C"?

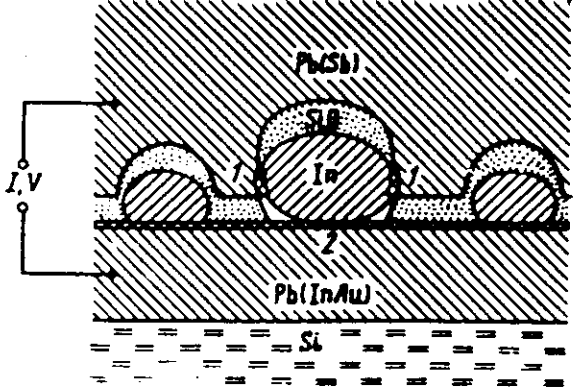

FIG. 1. Sectional diagram of the test structures.

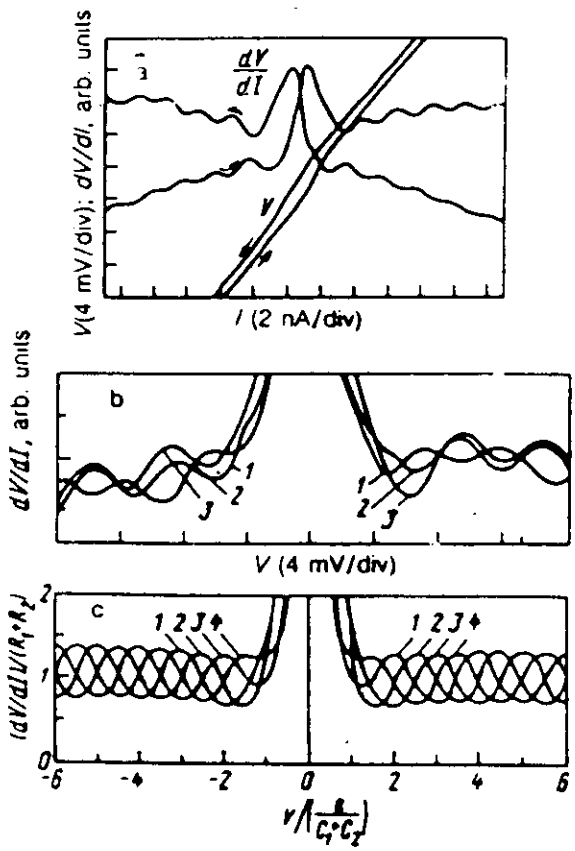

FIG. 2. The voltage V and the derivative dV/dI versus the current I or versus V. a: Experimental (Sample M 147-V). The average slope of the $R_d(I)$ curves and their shift upon the reversal of measurement direction are of instrumental origin. b: Three experiments with the same sample at $T = 4.2$ K, alternated with cycles of heating the sample to $T \approx 300$ K. c: Theoretical predictions. 1—$Q_0/e = 0$; 2—0.25; 3—0.5, 4—0.75 ($C_2/C_1 = 1$).

Recent observation

Tunneling through single grain.

Kuzmin and Likharev, JETP Lett. 45, 495 (1987)

← offset in I-V curve modulations

Heating and cooling changes modulation phase; period same. Amount of "trapped" charges on granules change

← theory of modulations

Technology helps increase Coulomb Blockade!

(Fulton and Dolan '87)

Need $\frac{e^2}{2C} > k_B T$ $\quad C \propto$ Junction area

Electron Beam Lithography $\rightarrow$ $A \lesssim 0.006\ (\mu m)^2$

$C \sim 0.2\ fF$

$\frac{e^2}{2C} \sim 0.4\ meV$

(Al/AlO/Al)

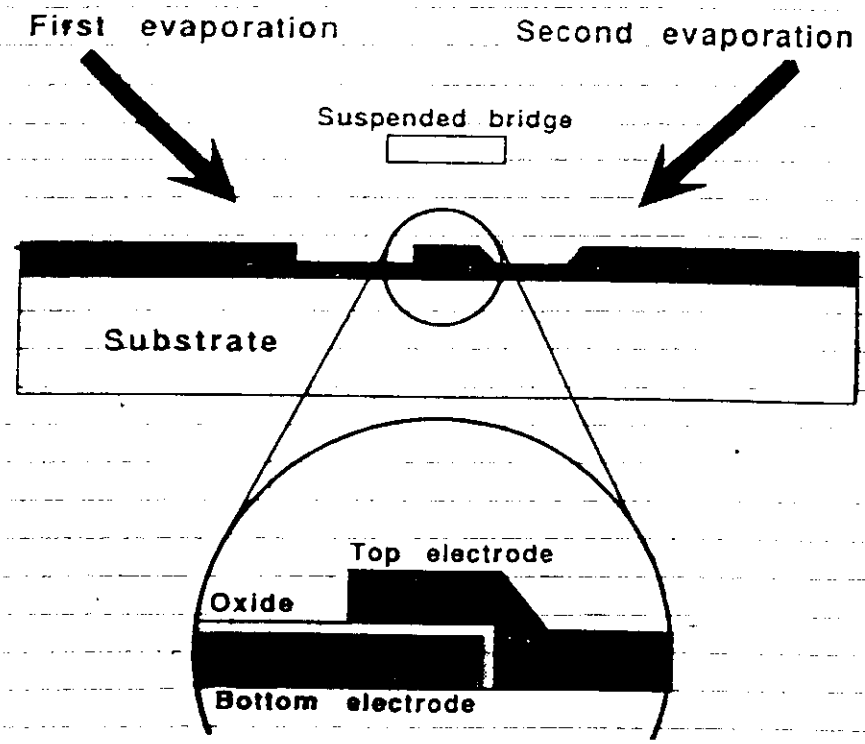

Fig. 4.1 The Dolan bridge technique.

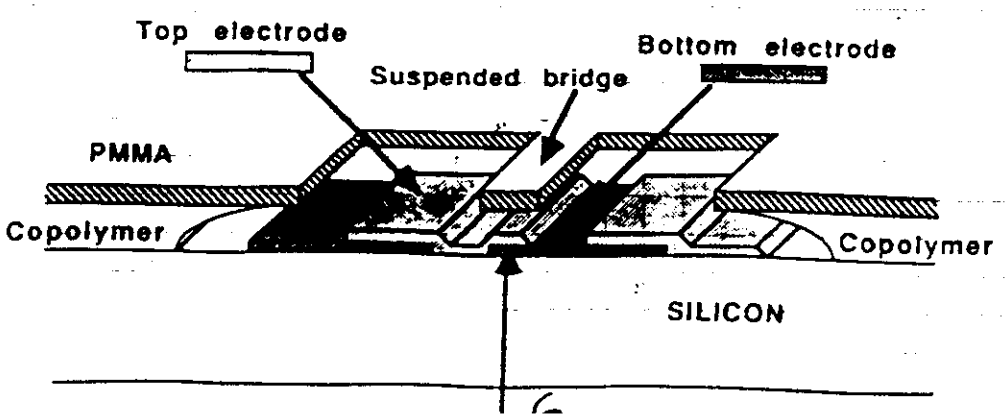

Recent Experiment

Fulton and Dolan, Phys. Rev. Lett. 59, 109 (1987)

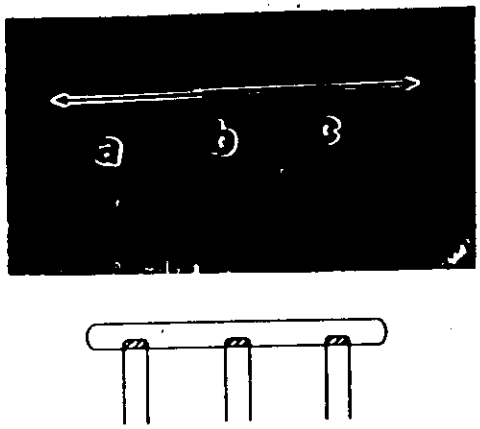

FIG. 2. A scanning-electron micrograph of a typical sample. Junctions labeled a, b, and c are formed where the vertical electrodes overlap and contact the longer horizontal central electrode. The bar is 1 μm long. The configuration is also shown in the accompanying drawing.

Note inset: $V_{offset} \propto (Area)^{-1}$

implies $V_{offset} = \frac{e}{2C}$ as $C \propto Area$

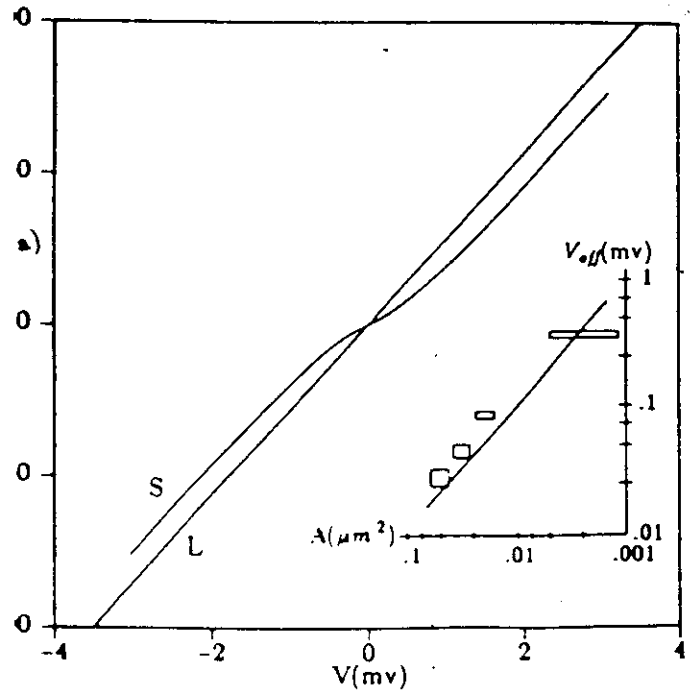

3. I-V curves S and L for junctions corresponding to ind large C at 1.7 K. Inset: Offset voltage vs junction as determined from scanning-electron-microscopy pho- ns) for four different samples. The boxes represent the ed uncertainties.

Different curves for different gate voltages (changes "zero" of charge on the strip)

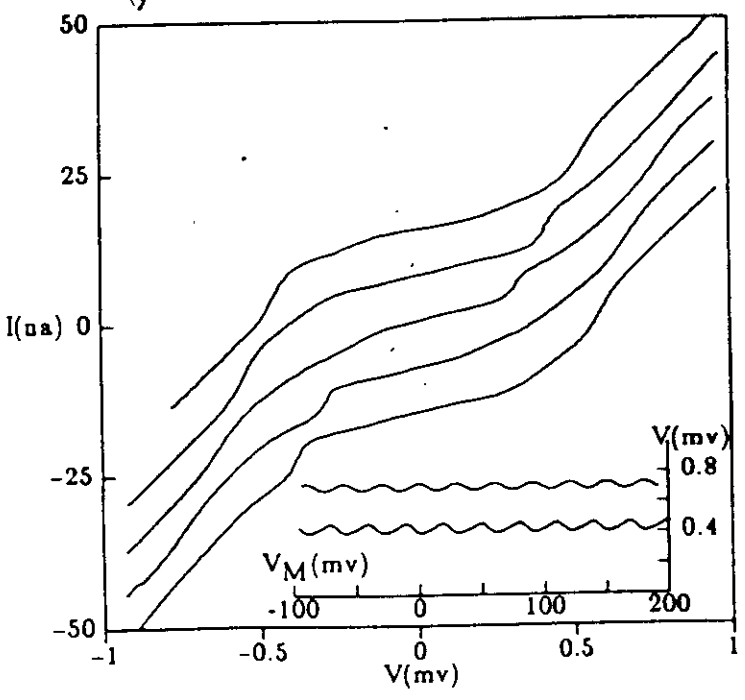

FIG. 5. I-V curves for a sample at $T = 1.1$ K for a set of equally spaced substrate biases covering $\frac{1}{6}$ of a cycle. Curves are offset by increments of 7.5 nA. Inset: V vs V_M for two fixed currents $I = 10.5$ and 26 nA.

Note modulation effect by substrate Bias V_m

I ... (inset)

Digression: "Principle" of transistor action in double junction
(Gate controlled tunneling)

I.O. Kulik and R.I. Shekhter, JETP 41, 308 (1975)

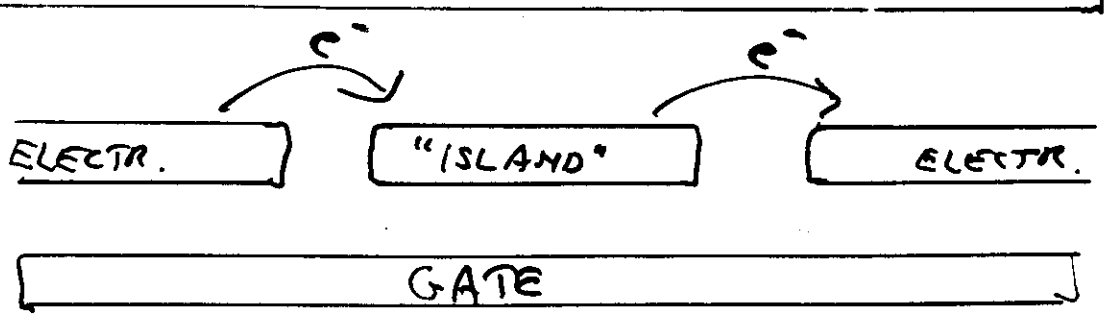

The Coulomb energy on the central electrode is

$$E_c = (e^2/2C)\,(n_1 - n_0)^2 + e\,(n_1 - n_0)\,\phi$$

n_0: equilibr. density

ϕ: electrostatic potential induced by gate

Rewrite by "completing the square"

DISCRETE → n_1 ; CONTINUOUS → $C\phi/e$

$$E_c = (e^2/2C)\,(n_1 - n_0 + C\phi/e)^2 - (C\phi/e)^2$$

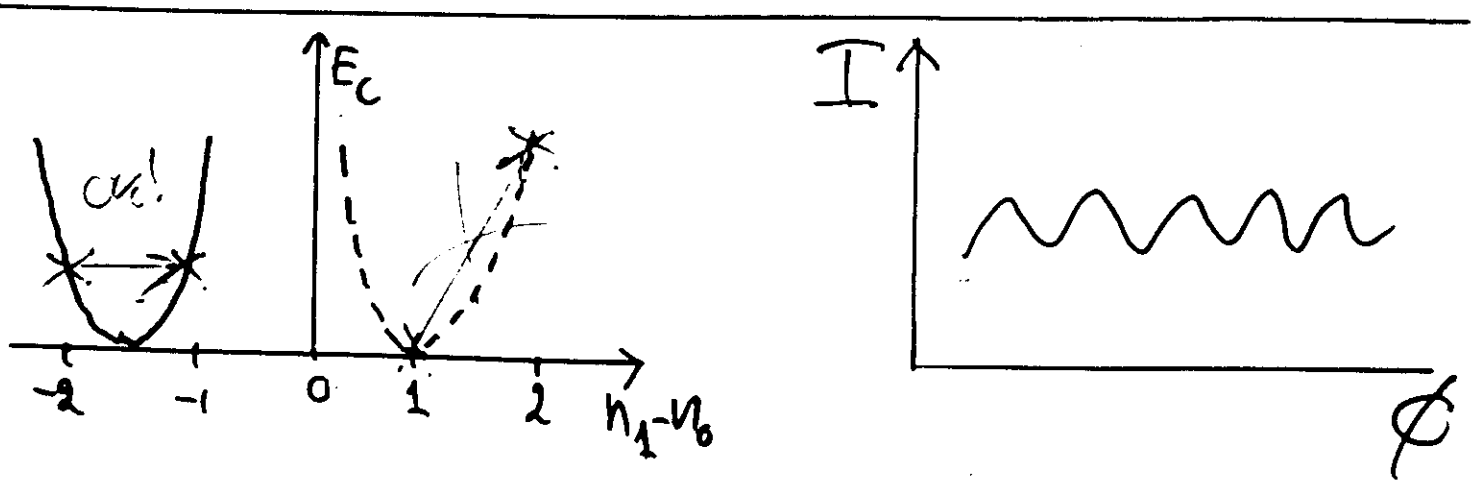

Depending on ϕ, Ec can be degenerate or nondegenerate w.r.t # electrons on island. Current changes periodically in ϕ.

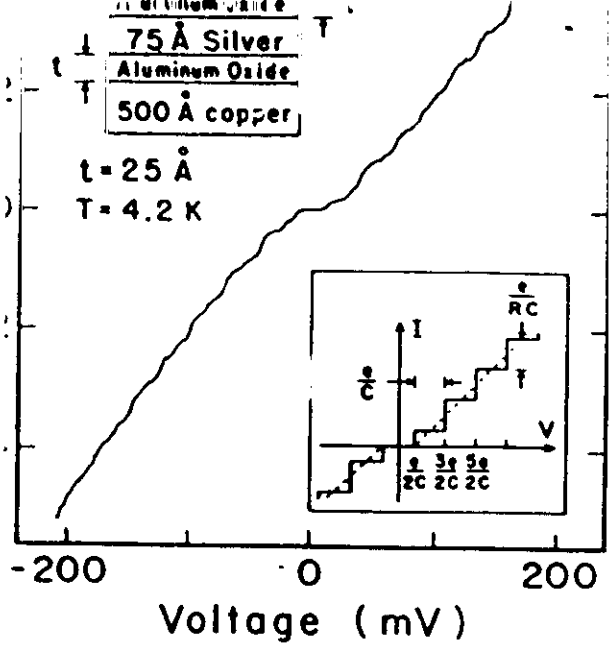

urrent-voltage characteristics taken with a voltage tunnel system where tunneling occurs into an iso- f silver particles 75 Å on average in diameter (see h the expected offset in the curve at zero bias (for es) by an amount $e/2c$—the "Coulomb gap"—and steps separated by a voltage e/C—the so-called aircase"—are evident in this trace. Also observed ıding current steps of magnitude e/RC. The mea- ɔf the steps is 0.72 nA, and the junction resistance This is consistent with the measured e/C voltage 7 mV (see Fig. 3). The inset shows an idealized ın of the current-voltage characteristic expected

Barner and Ruggiero,
Phys. Rev. Lett. 59, 807 (1987)

modulations

"Coulomb staircase"

current depends on # of excess electrons on central electrode (silver particle)

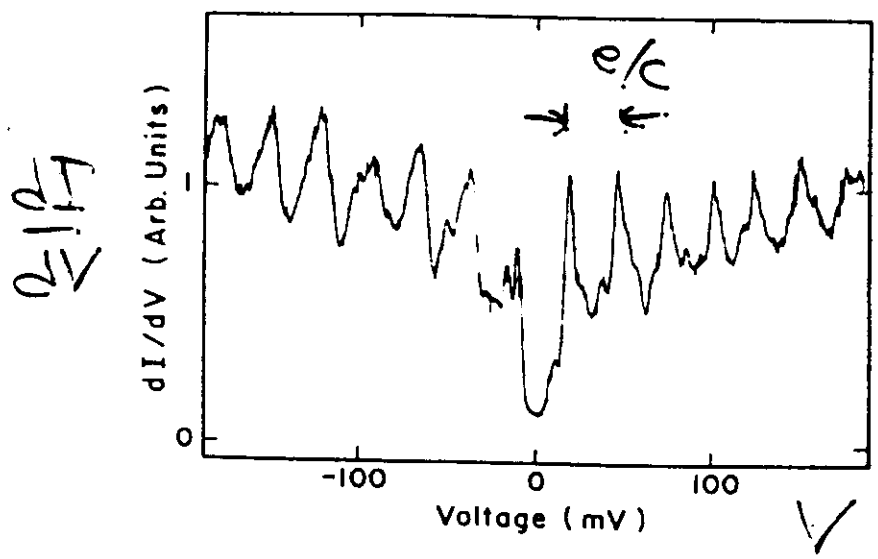

FIG. 3. Conductance trace (dI/dV vs V) accentuating the structure shown in Fig. 2. Here we see, beginning at zero bias, the gap of $e/2C$ in voltage, followed by a series of peaks separated by a voltage of $e/C = 27$ mV. The latter are clear manifestation of the so-called Coulomb staircase expected for tunneling into particles with ultrasmall capacitance. The Ag particles accept a single additional electron each time a peak is

Effect of High-Frequency Electrodynamic Environment on the Single-Electron Tunneling in Ultrasmall Junctions

P. Delsing,[1] K. K. Likharev,[1,2] L. S. Kuzmin,[1,2] and T. Claeson[1]

[1]*Department of Physics, Chalmers University of Technology, S-412 96 Göteborg, Sweden*

[2]*Department of Physics, Moscow State University, Moscow 119899 GSP, U.S.S.R.*

(Received 28 April 1989)

Single-electron tunneling in $Al/Al_xO_y/Al$ junctions with areas below 0.01 μm^2 was studied at temperatures close to 1 K. The junctions, placed in different high-frequency environments but similar in all other aspects, exhibited different dc I-V curves, in accordance with the theory of correlated single-electron tunneling. Our results imply that a tunneling electron can effectively probe its electrodynamic environment at distances much larger than cr_t, where r_t is the "traversal" time of its passage through the energy barrier.

PACS numbers: 74.50.+r, 73.40.Gk, 73.40.Rw

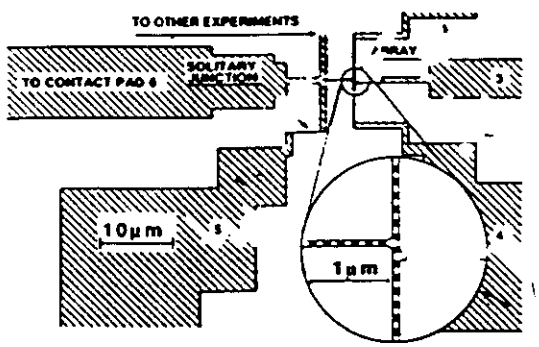

FIG. 1. Configuration of our thin-film structure. The schematically shown array region is blown up. A region which yields the largest contribution to the capacitance C_L between the solitary junction leads is marked gray.

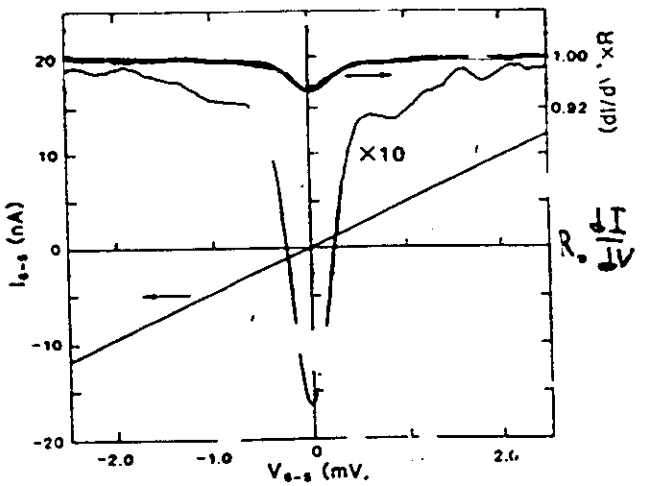

FIG. 3. dc current and differential conductance vs dc voltage for the solitary junction of the same sample and at the same temperature as in Fig. 2. The raised curve for the conductance is offset vertically to approach same horizontal asymptote at large voltages as the original curve.

solitary junction : small blockade

middle junction in array of junctions: large blockade

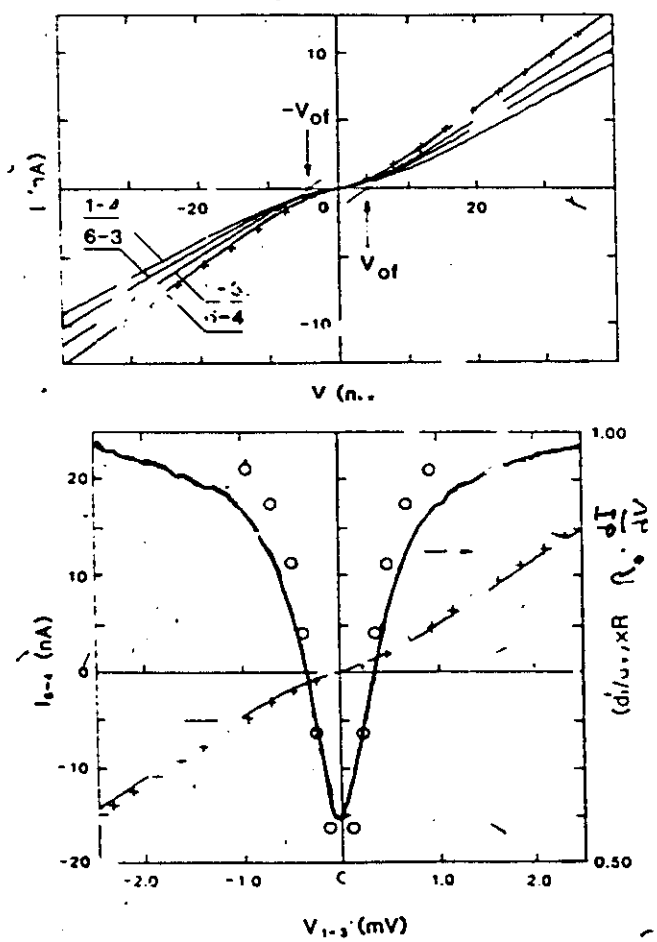

FIG. 2. I-V and dI/dV vs V for (a) various branches of 2D array and (b) the middle junction of the array. Indices show numbers of the contact pads. Solid lines: experimental curves. Thin lines: asymptotes of one of the I-V curves, showing definition of the offset voltage. Crosses and circles: results of a numerical simulation (Ref. 13) of the dynamics of thirteen-junction 1D array with parameters: $C_j = 2.0\times10^{-15}$ F, $R_j = 212$ kΩ (for $j=7$), $C_7 = 2.0\times10^{-16}$ F, $R_7 = 150$ kΩ, $(C_0)_{1,7} = 0.2\times10^{-16}$ F (for $i \neq 7$), $(C_0)_6 = (C_0)_7 = 0.6\times10^{-16}$ F, $T = 1.31$ K.

SEMICLASSICAL COULOMB BLOCKADE

Theory: Mullen et al. PRB 37, 98 (1988)
Averin and Likharev, J. Low. Temp. Phys. 62, 345 (1986)
...

Capacitance C
Tunneling (junct.) resistance R_J

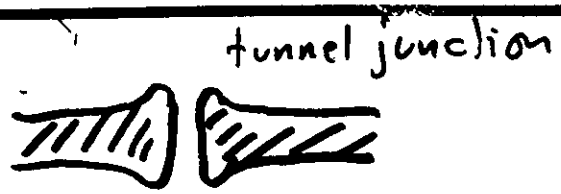

Apply a voltage

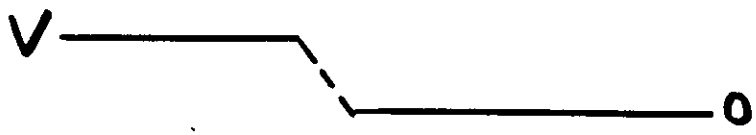

Charge before tunneling (continuous charge buildup)

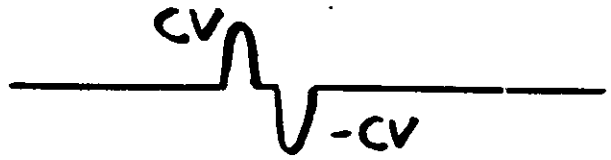

Charge after tunneling (discrete charge transfer)

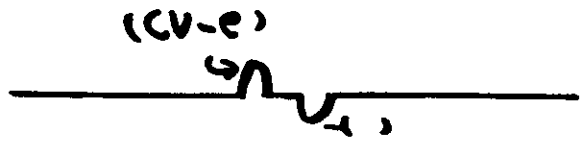

Change in energy = $eV - e^2/2C < 0$ unless $V > V_{th} = e/2C$

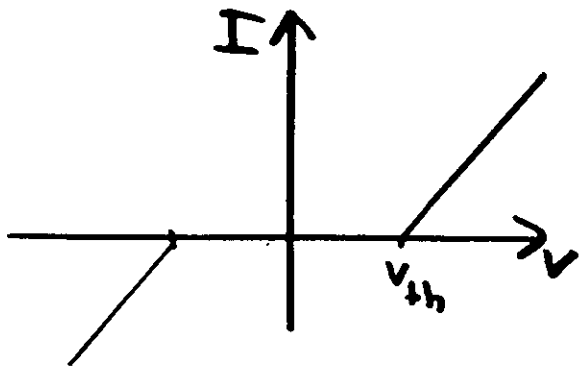

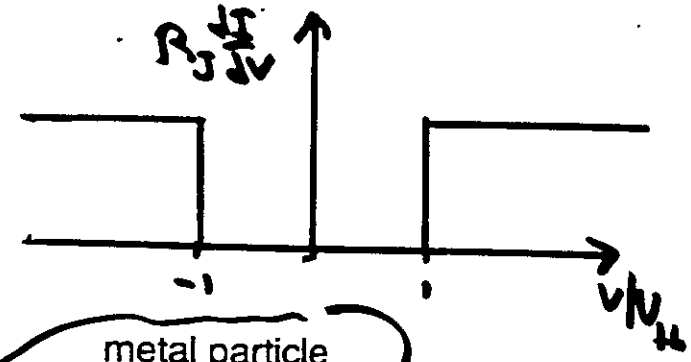

Experiments: Dolan and Fulton
Kuzmin
...

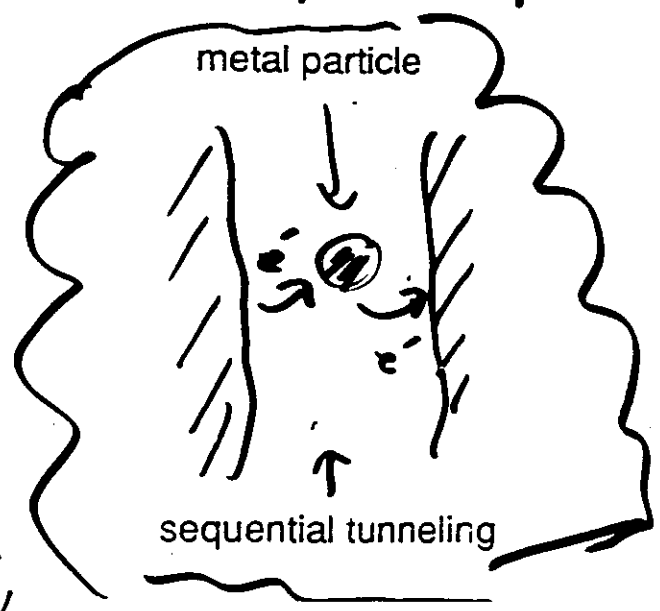

Sketch of semiclassical theory for Current biased Single Junction

$$I = \frac{e}{\tau} = \frac{V}{R} \Rightarrow \frac{1}{\tau} = \frac{eV}{e^2R}$$ (no blockade)

$\frac{1}{\tau}$: tunnel rate

eV: eV is energy gain

Blockade means energy gain: $eV \to eV - \frac{e^2}{2C}$

Assume:

$$\frac{1}{\tau(V)} = \Theta\left[eV - \frac{e^2}{2C}\right]\left[eV - \frac{e^2}{2C}\right]\frac{1}{e^2R} \; ; \; V(t) = \frac{It}{C}$$

impose fixed I, calculate $\overline{V(t)}$

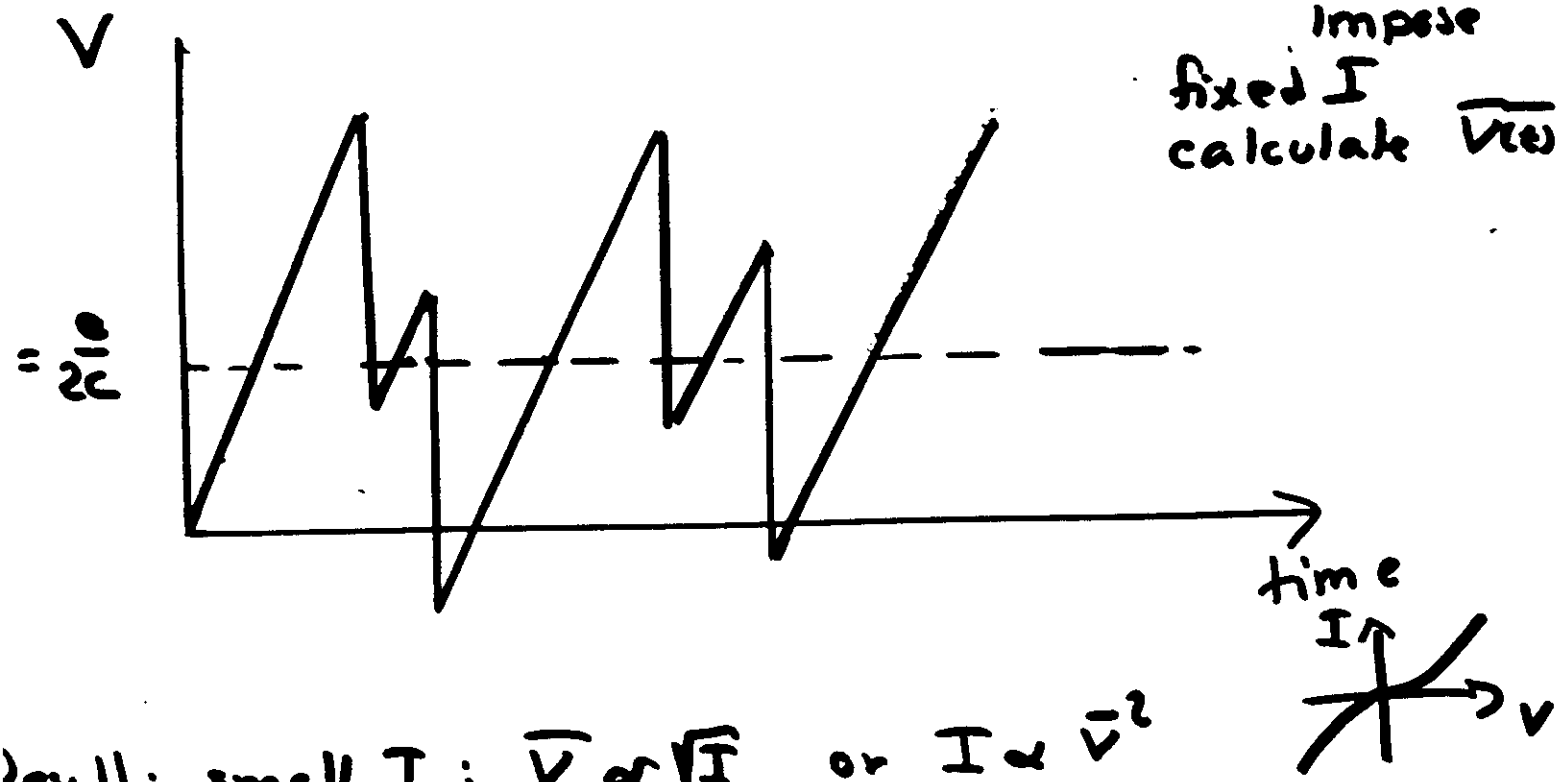

Result: small I: $\overline{V} \propto \sqrt{I}$ or $I \propto \overline{V}^2$

large I: $I = \frac{1}{R}\left[\overline{V} - \frac{e}{2C}\right]$ ("offset")

COMPLICATIONS: DISCHARGE

(tunneling through oxides is taken to be instantaneous)

- Leads modelled as transmission lines of impedance Z ($=\sqrt{L/C}$ if ideal)

- Consider no applied voltage

Charge before tunneling

Charge immediately after tunneling

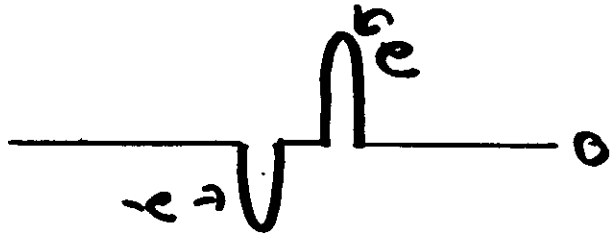

Energy: $\frac{e^2}{2C}$

- Very fast screening: Excess charge decouples from tunneling electron and discharges down leads

Charge on junction is

$q(0,t) \doteq e \exp(-t/\tau_D)$

$\tau_D = ZC$

- Uncertainty relation

$E_C / (h/\tau_D) = Z/[2 (h/e^2)] = Z/2R_H$ ← Parameter that will determine strength of blockade

NEED QUANTUM TREATMENT OF DISCHARGE

The degrees of freedom of the many-body system separates into <u>microscopic</u> single-particle modes and <u>macroscopic</u> collective (electromagnetic) modes

The total charge on the tunnel-junction is

$$q_{tot} = (n \cdot e + q_0)$$

microscopic "fermionic" charge (discrete in "e")

macroscopic collective ("bosonic") polarization charge (continuous)

The electrons (single-part. modes) are treated as non-interacting particles that only couple to the collective electromagnetic modes when they transfer a unit of charge across the junction

The coupling between single-particle and collective modes comes from the potential energy stored in the junction

$$U = \frac{(ne + q_0)^2}{2C}$$

Single junction with "quantum fluctuations"

Most of the physics in this "toy model":

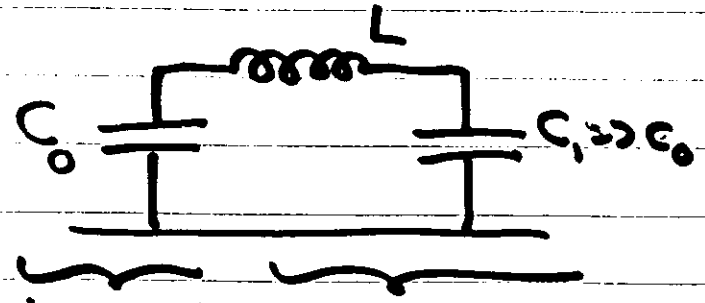

The impedance L delays the removal of a tunneled electron

Classically after tunnel event : $V(t) = \frac{e^2}{2C_0} e^{-t/\tau_D}$

τ_D large → strong blockade $\quad \tau_D = C_0 Z$

τ_D small → weak -"-. $\quad Z$ ↑ impedance of T.L.

crossover for $\hbar/\tau_D = \frac{e^2}{2C_0}$

or $Z \sim \frac{1}{\pi} R_H \sim 8\,k\Omega$

The classical Hamiltonian is

$$\mathcal{H}(\dot{q}, q) = \underbrace{\frac{L}{2}\dot{q}^2 + \frac{1}{2C} q^2}_{\text{harmonic oscillator! quantize!!}} + E_{\text{const}} \quad : \quad q = q_0 - \bar{q}_0$$

"$L \leftrightarrow m$", "$\frac{1}{C} \leftrightarrow m\omega^2$" $\rightarrow \omega = \frac{1}{\sqrt{LC}} \rightarrow \epsilon_n = (n+\frac{1}{2})\hbar\omega$

$\{\psi_n\}$ known

After tunneling $q = e$! (sudden approx. OK)

Hence initial state (before tunneling) of T.L.

$$\psi_i(q) = \psi_0(q)$$

↳ h.o. ground state w.f.

Final state (after tunneling)

$$\psi_f(q) = \psi_0(q+e)$$

corresponding to a displaced harmonic oscillator.
There is a finite probability P_0 to remain in the ground state (cf. Mössbauer)

$$P_0 = |\langle \psi_i | \psi_f \rangle|^2 = e^{-W} \quad ; \; W = \pi^2/R_H$$

$$P_n = \frac{W^n e^{-W}}{n!}$$

Current is easily calculated: $I = \frac{1}{eR} \sum_{n=0}^{\infty} \frac{W^n}{n!} e^{-W} [eV - n\omega] \cdot \Theta(eV - n\omega)$

large V: $I \to \frac{1}{eR}\left[eV - \frac{e^2}{2C}\right]$ (= "offset")

Small V: $I \to \frac{1}{eR} e^{-W} \cdot V \qquad W \sim \frac{\pi}{8h\Omega}$

$\sqrt{\langle q^2 \rangle}$ size of quantum in the ground state

δq (displacement)

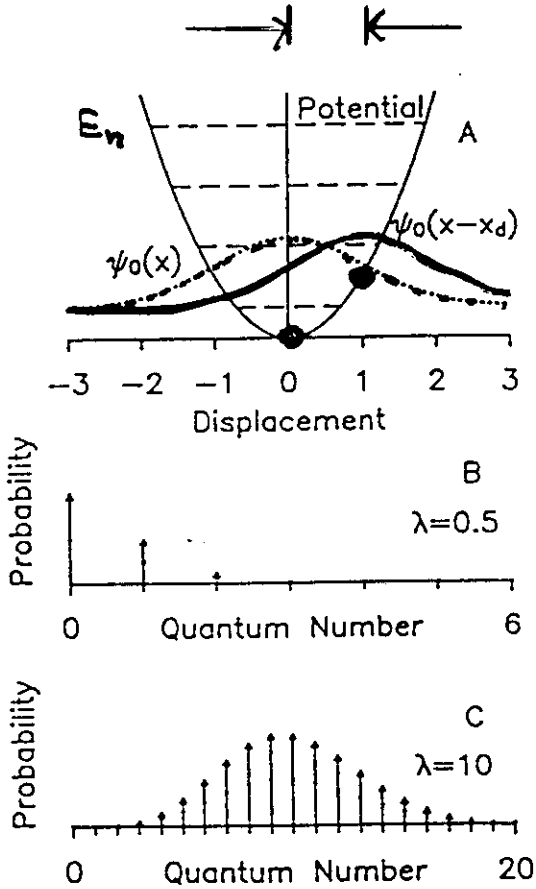

Fig.1 Suddenly displaced harmonic oscillators. Panel A shows a harmonic potential and the effect of being displaced on classical and quantum particles moving in this potential. When a classical particle in its ground state (open circle) is displaced (closed circle) it still has a well defined energy. When a quantum particle in its ground state (dotted line) is displaced (solid line) its energy is no longer well defined as it is a superposition of all of the eigenstates of the oscillator, each with its own energy (dashed lines). Panels B and C show the probability distribution over the different harmonic oscillator states when an oscillator is slightly and strongly displaced respectively.

$$\lambda = \frac{(\delta q)^2}{4\langle q^2 \rangle} = \frac{e^2/2C_0}{\hbar\omega}$$

$$P_n = e^{-\lambda}\lambda^n/n!$$

$$\bar{n} = \sum_n n P_n = \lambda$$

$$\bar{E} = \sum_n n\hbar\omega P_n = \frac{e^2}{2C_0}$$

$$\overline{(\Delta E)^2} = \sqrt{\frac{e^2}{2C_0}\cdot\hbar\omega}$$

① Note: Classical limit $\hbar \to 0 \Rightarrow \bar{n} \to \infty$, $\overline{(\Delta E)^2} \to 0$ and P_n has sharp peak at $e^2/2C_0$.

② Note: $\bar{n} \to \infty$ also as $\omega \to 0$

$\Rightarrow$ "Orthogonality Catastrophe" and gives power law behavior of $dI/dV \sim V^{\beta}$ as $V \to 0$

MODEL

(similar model studied by Nazarov; Devoret et al.)

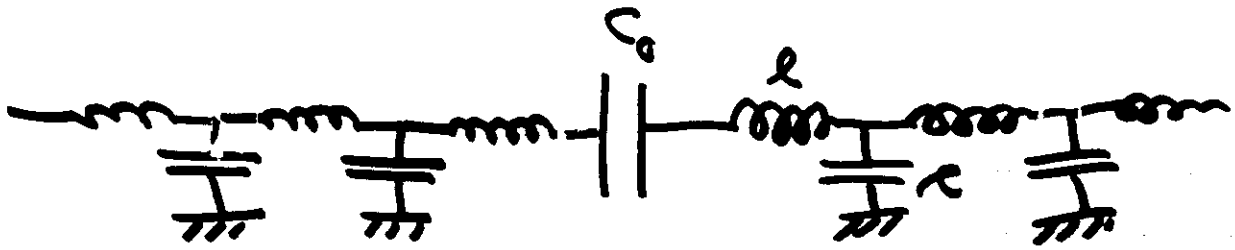

$$= \sum_i \epsilon_{Li} c_i^\dagger c_i + \sum_j \epsilon_{Rj} d_j^\dagger d_j$$

left + right non-interacting electron baths

$$+ \sum_k \omega_k a_k^\dagger a_k \begin{cases} \frac{1}{2C_0} q_0^2 \\ \sum_n \frac{1}{2C} q_n^2 \\ \sum_m \frac{L}{2} j_m^2 \end{cases}$$

junction charging energy

capacitance of leads

inductance of leads

$$+ \sum_{ij} T_{ij} c_i^\dagger d_j e^{ie\phi_0} + H.c.$$

tunneling term

Use first order perturbation theory (in T_{ij}):

Initial State $\left| \text{Left Fermi sea at raised voltage} \right\rangle \left| \text{Right Fermi sea} \right\rangle \left| \text{Boson ground state} \right\rangle$

Final State $c_i |LFS\rangle \, d_j^\dagger |RFS\rangle \, |\{n_k\}\rangle$

SINGLE ELECTRON TRANSFER BUT ALL BOSON FINAL STATES

Classical time dependence of a charge suddenly placed on a junction connected to an ideal transmission line

To generalize single-oscillator model we project δq_0 onto the normal modes of the transm. line

$\lambda \to \{\lambda_k\}$

$\lambda_k = \dfrac{(\delta q_k)^2}{\langle q_k^2 \rangle}$

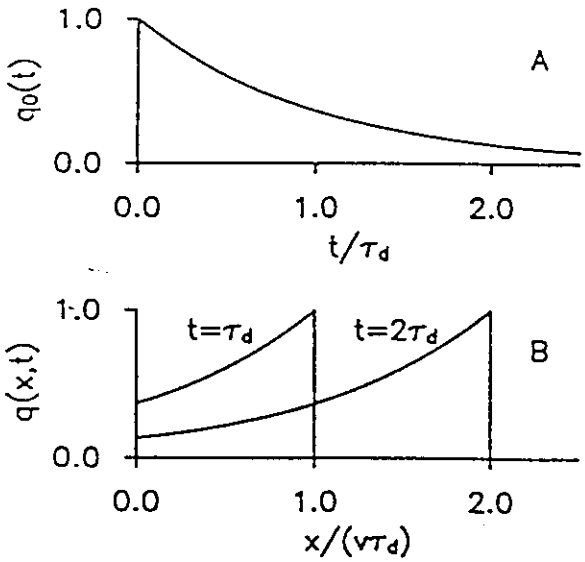

$\delta q_0(t)$

$\delta q(x,t)$

Fig.2 Classical time dependence of a charge suddenly placed on a junction connected to an ideal transmission line. Panel A shows the decay in time of the charge remaining on the junction and Panel B shows the classical charge wave propagating down the transmission line. The quantity $v = 1/\sqrt{lc}$ is the speed of light in the transmission line.

$$A(\omega) = 2\pi \sum_{\{n_k\}} \left[\prod_k e^{-\lambda_k} \frac{\lambda_k^{n_k}}{n_k!} \right] \delta\left(\omega - \sum_k n_k \omega_k\right) =$$

Spectral function for the e.m. modes

$$= \int_{-\infty}^{\infty} dt\, e^{i\omega t} \exp\left\{ \frac{e^2}{2C_0} \int_0^{\infty} \frac{d\nu}{2\pi}\, a(\nu) \left(\frac{e^{-i\nu t} - 1}{h\nu} \right) \right\}$$

$a(\nu)$ has to do with normal mode distr. in T.L. (classical)

$$a(\nu) = \mathrm{Re}\left[4 / \left(i\omega + 1/C_0 Z(\omega) \right) \right]$$

$Z(\omega)$ is impedance of the transmission line

Effect of exciting transmission line modes on the tunneling probability (and current)

$$I(V) = e\int_0^{eV}\frac{d\epsilon_L}{2\pi}\int_0^{eV}\frac{d\epsilon_R}{2\pi}\int_0^{\infty}\frac{d\omega}{2\pi}\,|T(\epsilon_L,\epsilon_R)|^2\,A(\omega)\,2\pi\,\delta(\epsilon_L-\epsilon_R-\omega)$$

- $|T(\epsilon_L,\epsilon_R)|^2$: electronic coupling
- $A(\omega)$: excitation distribution
- $\delta(\epsilon_L-\epsilon_R-\omega)$: energy conservation

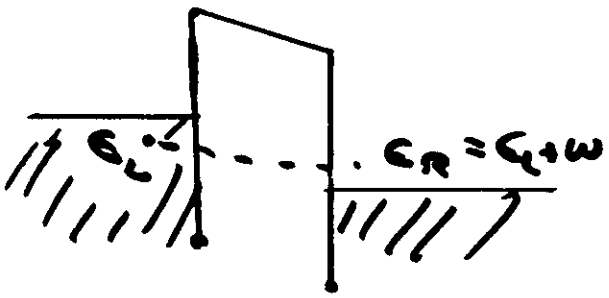

$$\frac{dI}{dV} = \frac{1}{R_J}\int_0^{eV}\frac{d\omega}{2\pi}A(\omega)$$

- $\frac{1}{R_J}$: bare tunneling resistance
- $\int_0^{eV}\frac{d\omega}{2\pi}A(\omega)$: probability that excitation has less energy than eV

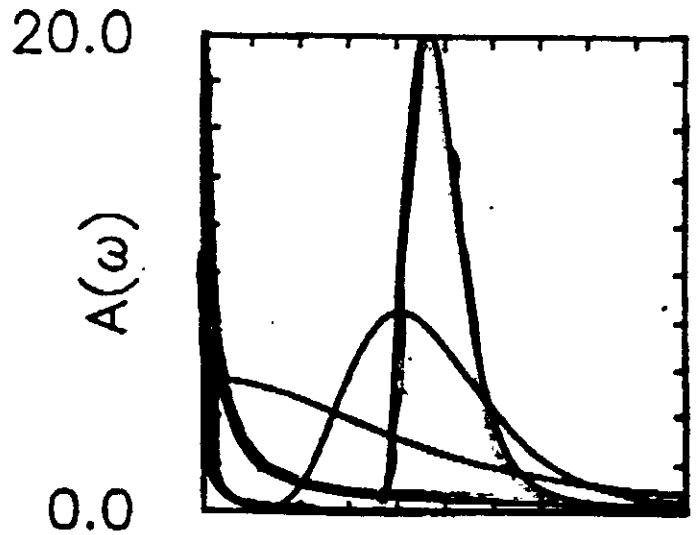

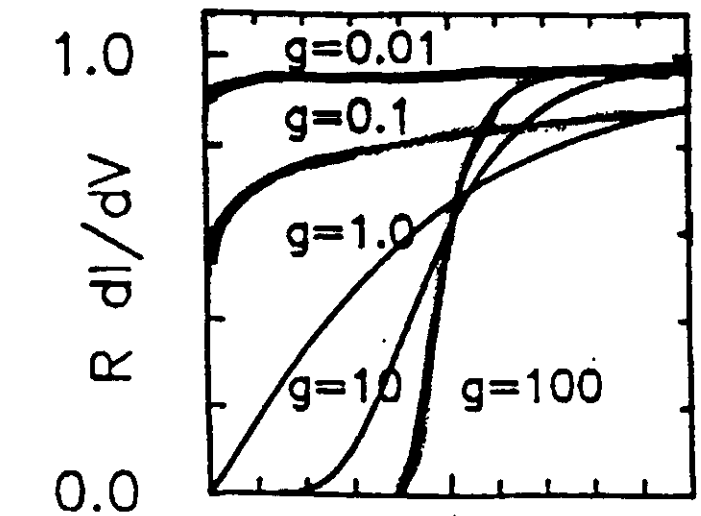

Ideal transmission lines

$$\left(g = \frac{2Z}{R_H}\right)$$

physical g's are ~0.02

($Z \sim 100\ \Omega$)

$$R_J\frac{dI}{dV} \sim V^g \quad \text{for small } g.$$

X-ray edge singularity in metallic Na.

(from Mahan: Many-Particle Physics p. 760)

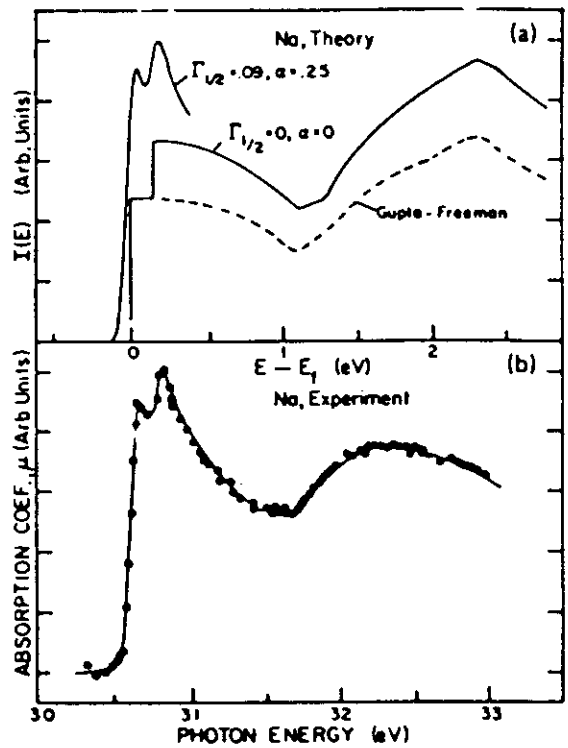

FIGURE 8.17. The X-ray absorption edge of the $L_{2,3}$ shell of metallic sodium. The data is shown in part (b). Part (a) shows how the band structure prediction of Gupta and Freeman is convoluted with the edge singularity ($\alpha = 0.25$) and broadening functions to fit the spectra. *Source*: Callcott *et al.* (1978) (used with permission).

TABLE 8.3. Orthogonality Index α

	Na	Mg	Al
Experiment[a]	0.20	0.13	0.12
Theories			
Minnhagen[b]	0.19	0.13	0.11
Almbladh–von Barth[c]	0.20		0.13
Bryant–Mahan[d]		0.12	0.10

[a] Citrin *et al.* (1977).
[b] Minnhagen (1977).
[c] Almbladh and von Barth (1976).
[d] Bryant and Mahan (1978).

Experimental comparison of single and multi-junction tunneling configurations

P. Delsing, K.K. Likharev, L.S. Kuzmin and T. Claeson
PRL 63, 1180 (1989)

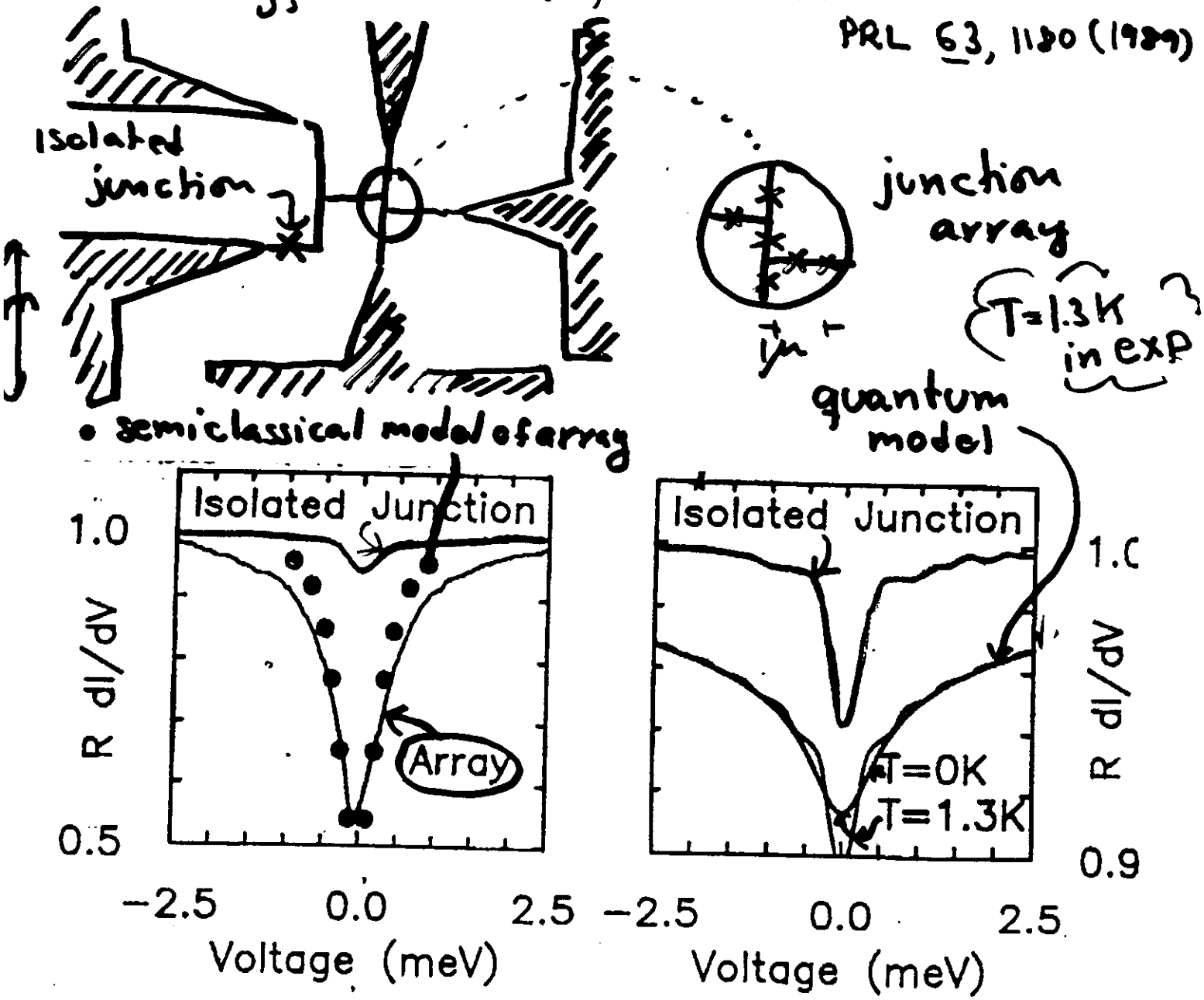

- Semiclassical model describes array (high impedance env., small q.m. fluct.)
- Quantum model approximately describes isolated junction (low impedance env.)

Comparison with Delsing's exp on isolated junction (enlargement)

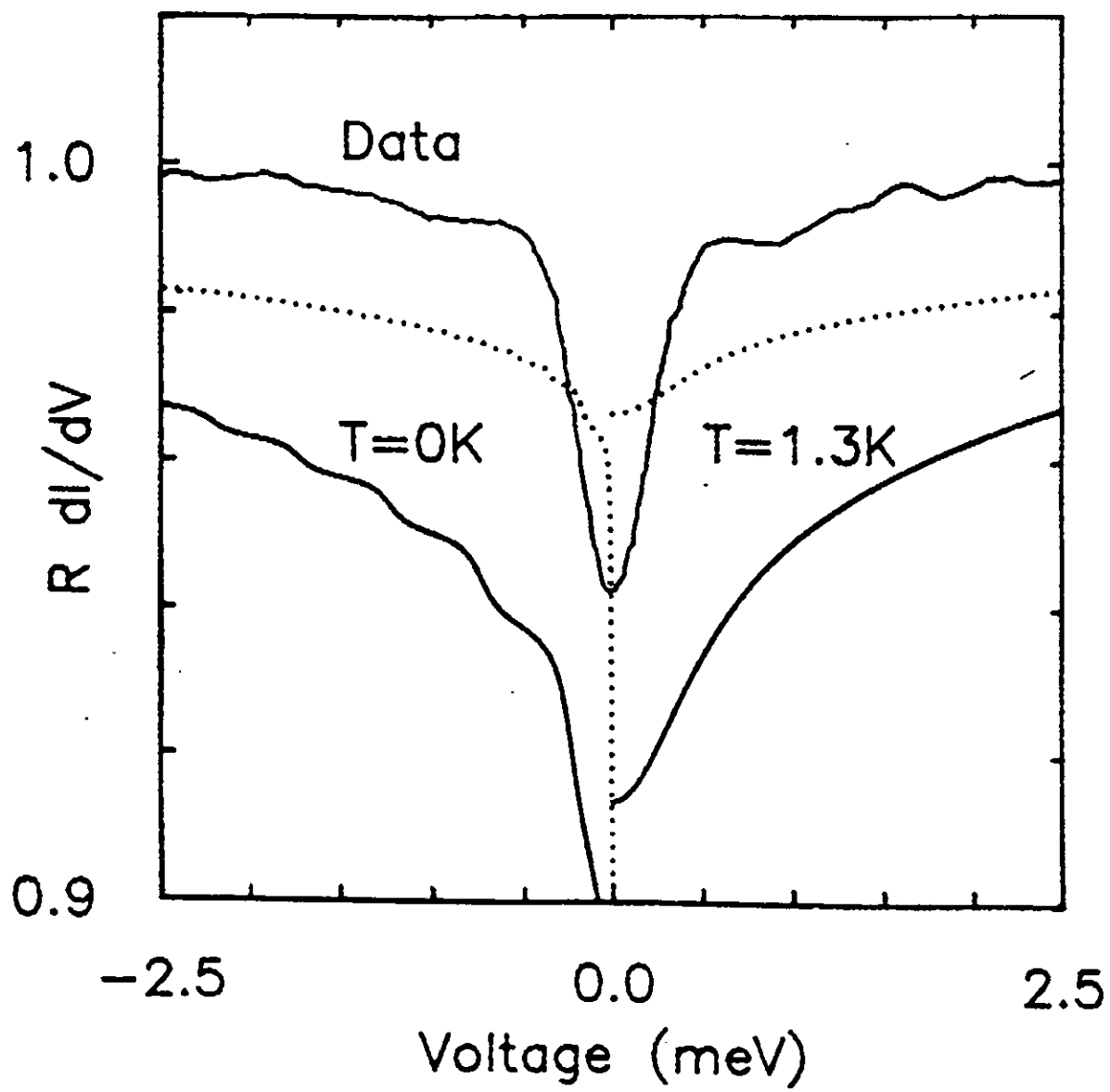

Consider fit to a different kind of experiment!

(indicates magnitude of quantum fluctuations underestim.?)

Crossed Pt-wires between adjustable-thickness (frozen) helium layer.

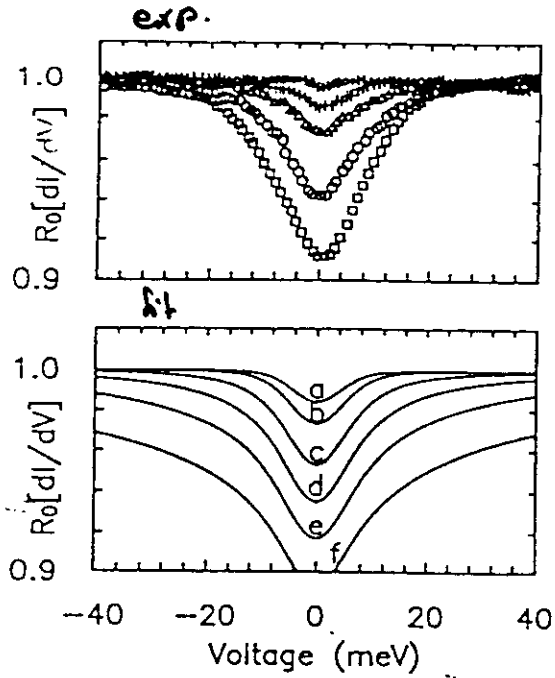

S. Gregory (unpublished!)

Fig.8 Comparison of theory and the measurements of Gregory [20]. The bottom panel shows the calculated conductivity of isolated junctions with a series of different charging energies (E_C= (a) 0.1, (b) 0.2, (c) 0.5, (d) 1.0, (e) 2.0, (f) 5.0 meV) plotted as a function of voltage. The details of the calculation are discussed in the text. The top panel shows the measured conductivity for five different junctions.

Fit to above theory by assuming $Z_{wires} = 2 \cdot Z_{free\ space}$

$$1.6 \cdot 10^{-17}\,F < C_0 < \frac{R_Q}{2\pi} \cdot 10^{-15}\,F$$

$$0.1\ meV < e^2/2C_0 < 5.0\ meV$$

caution: junction parameters not well known

"Good" fit to experiment only if T artificially raised from $T_{exp} = 4.2\,K$ to $20\,K$.

Need to include additional quant. fluctuations of charge across the junction?!

Charge Fluctuations in Small-Capacitance Junctions

A. N. Cleland, J. M. Schmidt, and John Clarke
Department of Physics, University of California, Berkeley, California 94720
and Materials and Chemical Sciences Division, Lawrence Berkeley Laboratories, Berkeley, California 94720
(Received 18 December 1989)

The current-voltage characteristics of submicron normal-metal tunnel junctions at millikelvin temperatures are observed to exhibit a sharp Coulomb blockade with high-resistance thin-film leads, but to be heavily smeared for low-resistance leads. As the temperature is lowered, the zero-bias differential resistance tends asymptotically to a limit that is greater for junctions with high-resistance leads. Both observations are explained in terms of a model in which quantum fluctuations in the external circuit enhance the low-temperature tunneling rate. The predictions are in reasonable agreement with the data.

PACS numbers: 74.50.+r, 05.30.−d, 73.40.Gk

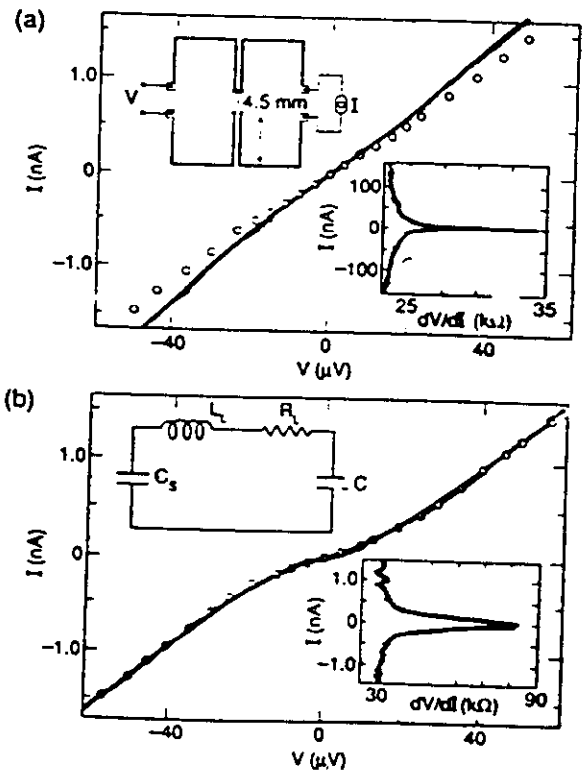

FIG. 1. *I-V* characteristics (solid lines) for two junctions at 20 mK with (a) $C=4\pm1$ fF and $R=23$ kΩ and (b) $C=5\pm1$ fF and $R=28$ kΩ. Dots represent predictions of theory. Inset in each figure is dV/dI vs I; note different current scales. Also inset in (a) is the configuration of junction and leads (not to scale) and in (b) its simplified representation.

V=0, temperature dependence of differential resistance

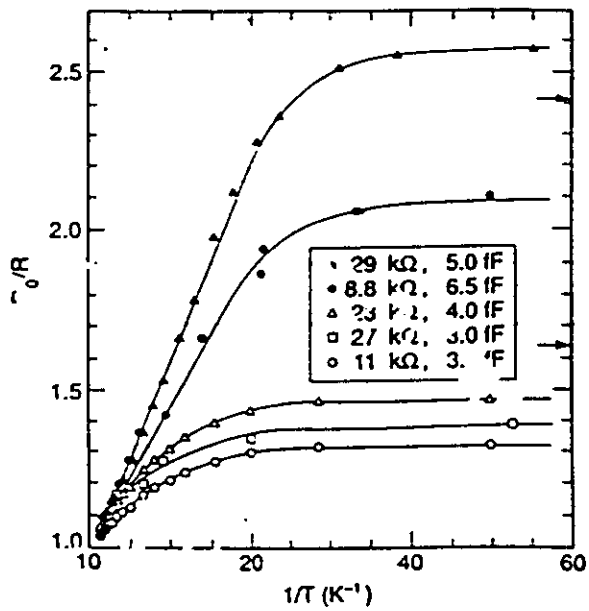

FIG. 2. R_0/R vs $1/T$ for five junctions; the open symbols are for low lead resistance and the solid symbols for high lead resistance. Arrows indicate the predicted values of R_0/R.

↑ Nominal resistance of tunnel junction matters also (not only 25

Resistive leads

Impedance $\simeq \sqrt{\frac{r}{\omega c}}$

- strong zero bias anomaly $R\frac{d^2I}{dV^2} \to \frac{1}{V^{3/2}} e^{-1/V}$ (no power law) as $V \to 0$
- long "tails" at large V solve by FFT

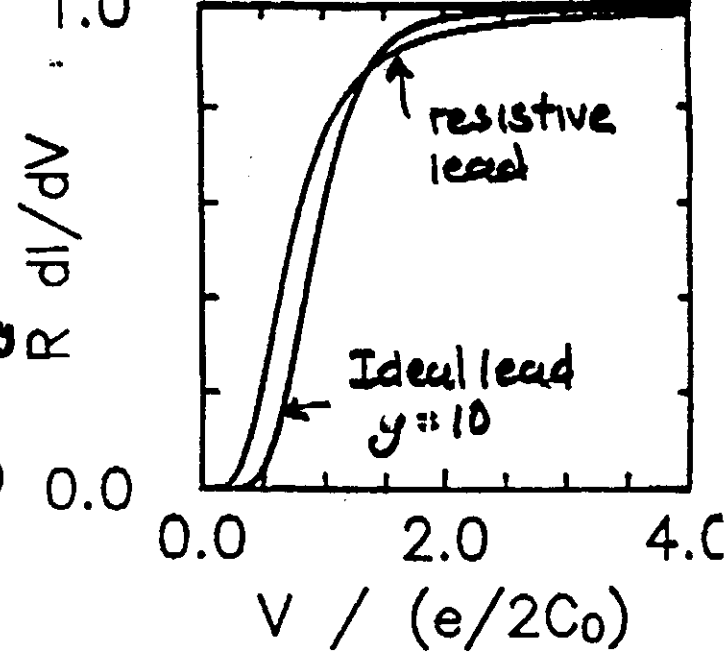

Finite temperatures

$$I(V,T) = \frac{1}{R_J}\int_{-\infty}^{\infty}\frac{d\omega}{2\pi}A(\omega,T)\int_{-\infty}^{\infty}d\epsilon\{n_F(\epsilon-eV)[1-n_F(\epsilon-\omega)] - n_F(\epsilon)[1-n_F(\epsilon-eV-\omega)]\}$$

$$A(\omega,T) = \int_{-\infty}^{\infty}dt\, e^{i\omega t}\exp\left\{\int_{-\infty}^{\infty}\frac{d\nu}{\nu}[e^{-i\nu t}-1][1+n_B(\nu)]\cdot \text{Bose factor}\right.$$

$$\left.\times \mathrm{Re}\left[\frac{2Z(\nu)}{R_H}\frac{1}{1+i\nu Z(\nu)}\right]\right\}$$

(impedance)

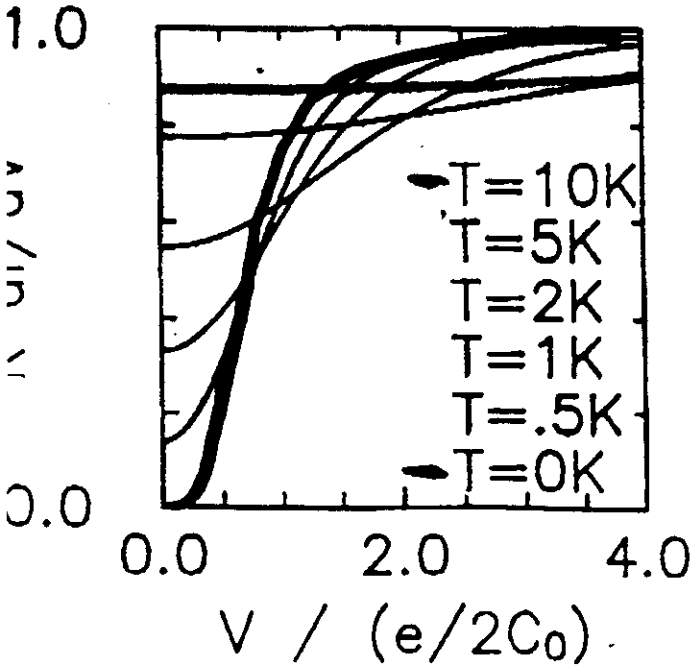

Temp. dep. of $R(0)^{-1} \equiv (dI/dV)_{V=0}$ contains signature of quantum behavior.

Resistive transmission lines

A.N. Cleland, J.M. Schmidt & John Clarke, PRL 64, 1565 (1989)

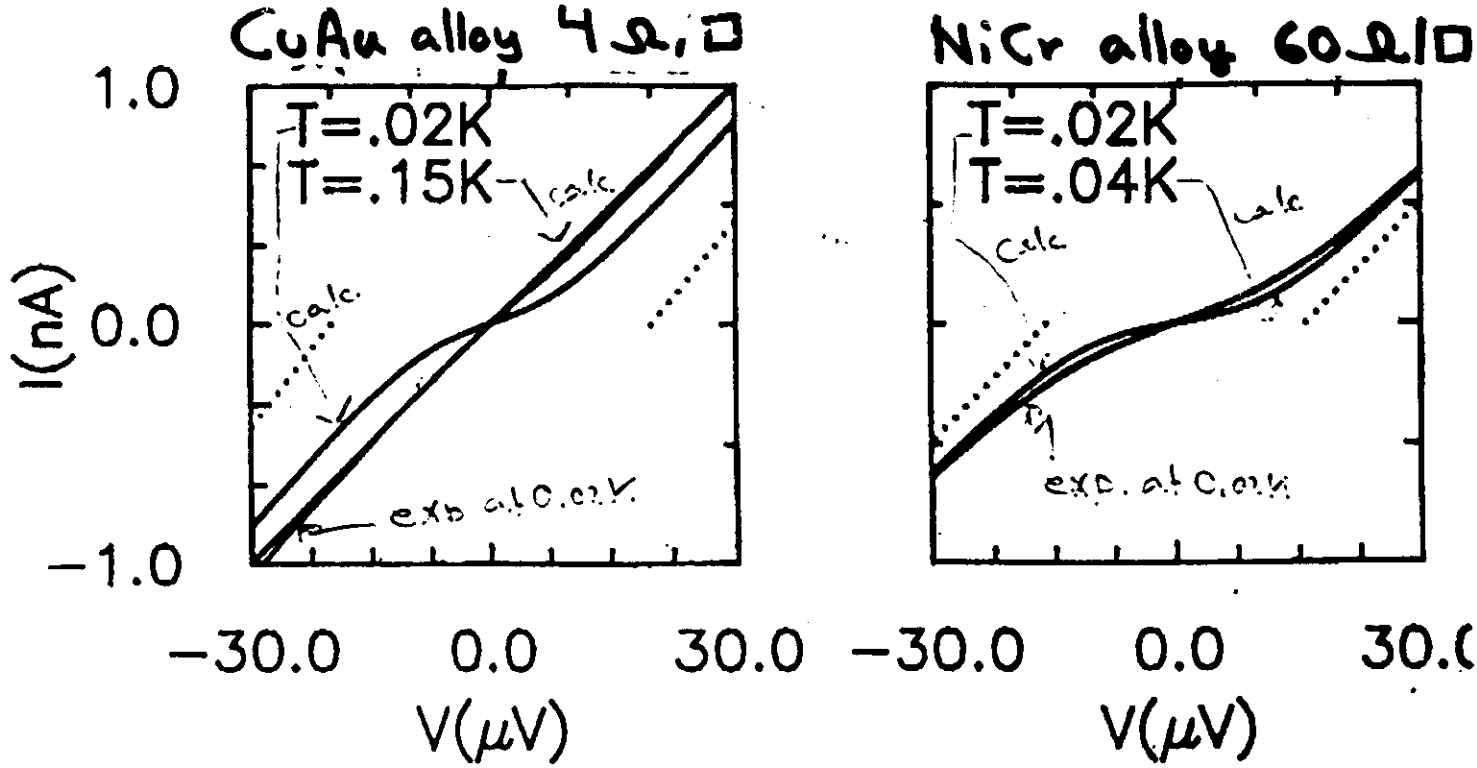

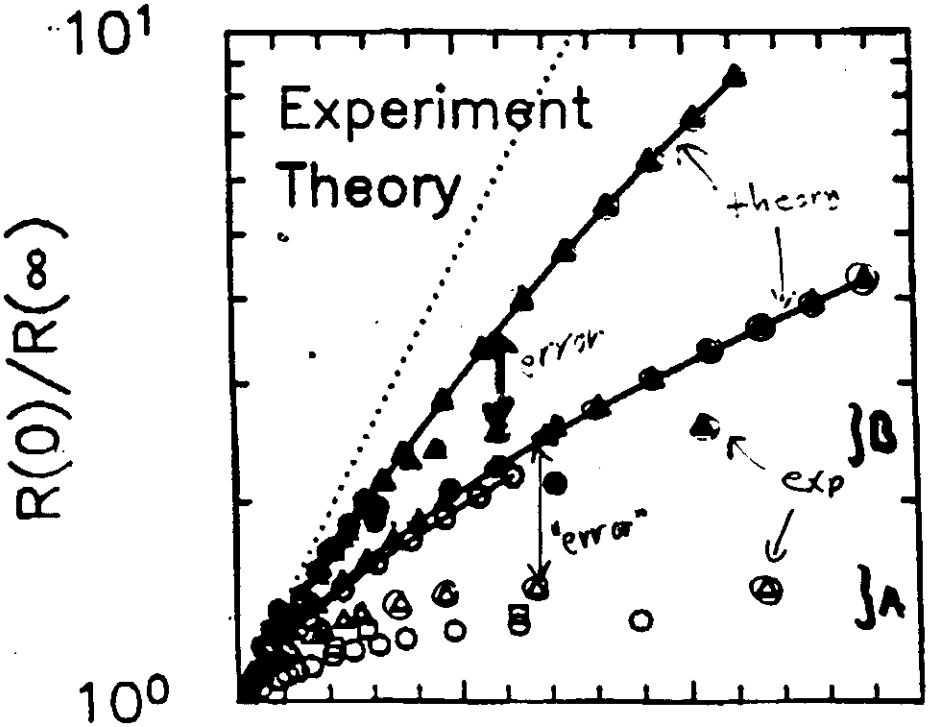

- Qualitative agreement at high temperatures
- no saturation in theory

○	11 kΩ, 3.0 fF	A
□	27 kΩ, 3.0 fF	A
△	23 kΩ, 4.0 fF	A
●	8.8 kΩ, 6.5 fF	B
▲	29 kΩ, 5.0 fF	B

junction param.

A-junctions with CuAu, B-junctions with NiCr leads

UNCONNECTED SYMBOLS: EXP

CONNECTED -"- : THEORY

FILLED SYMBOLS : HIGH RESISTANCE LEADS (N.C.)

OPEN SYMBOLS : LOW " , " (CuAu)

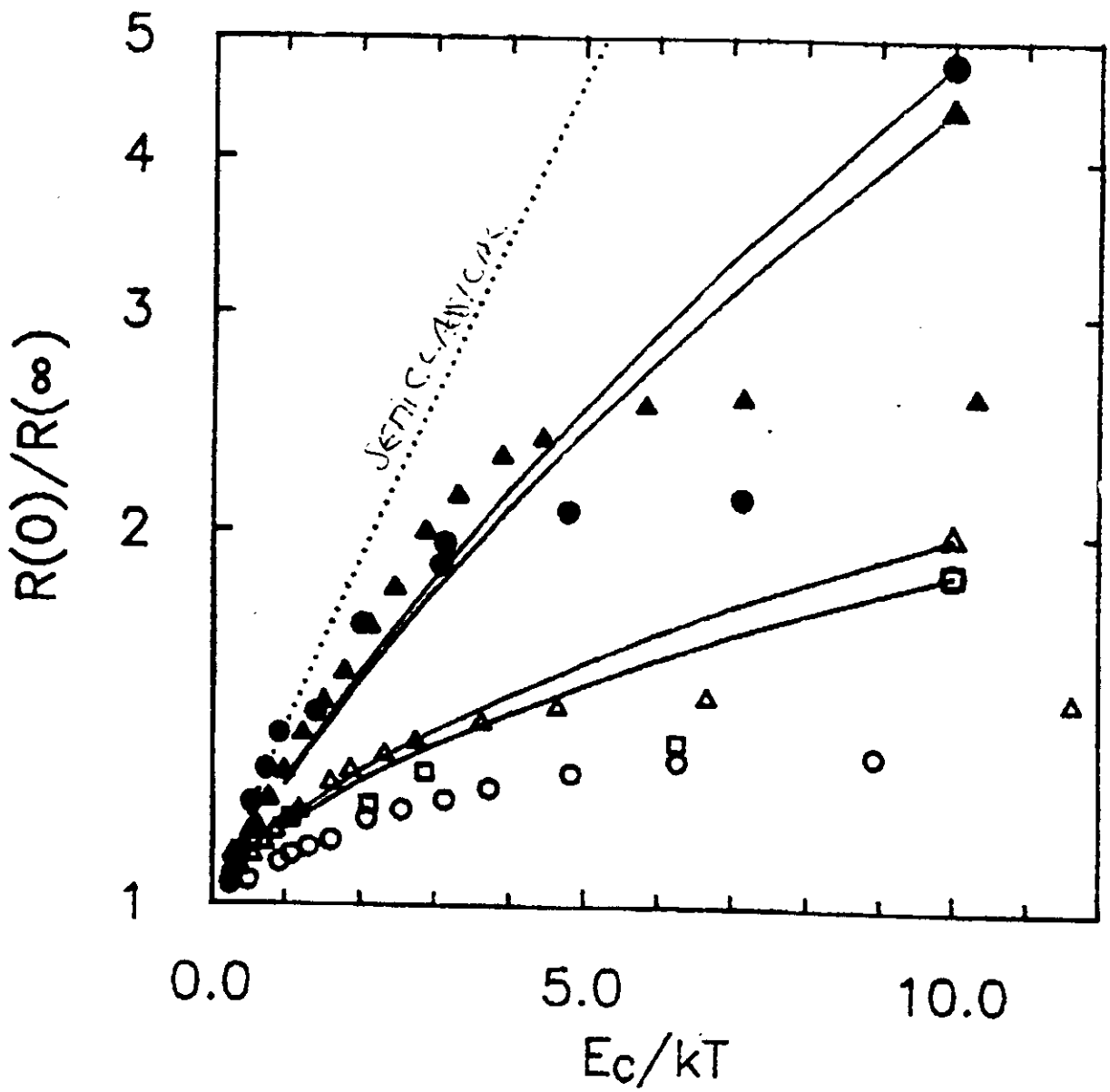

Comparison with exp of Cleland et. al.

with fluctuations across junction added in continuum ("spin-wave"-approximation)

$$\frac{1}{Z(\omega)} \rightarrow \frac{1}{Z(\omega)} + \frac{1}{R_J}$$

"improved agreement, but not good enough"

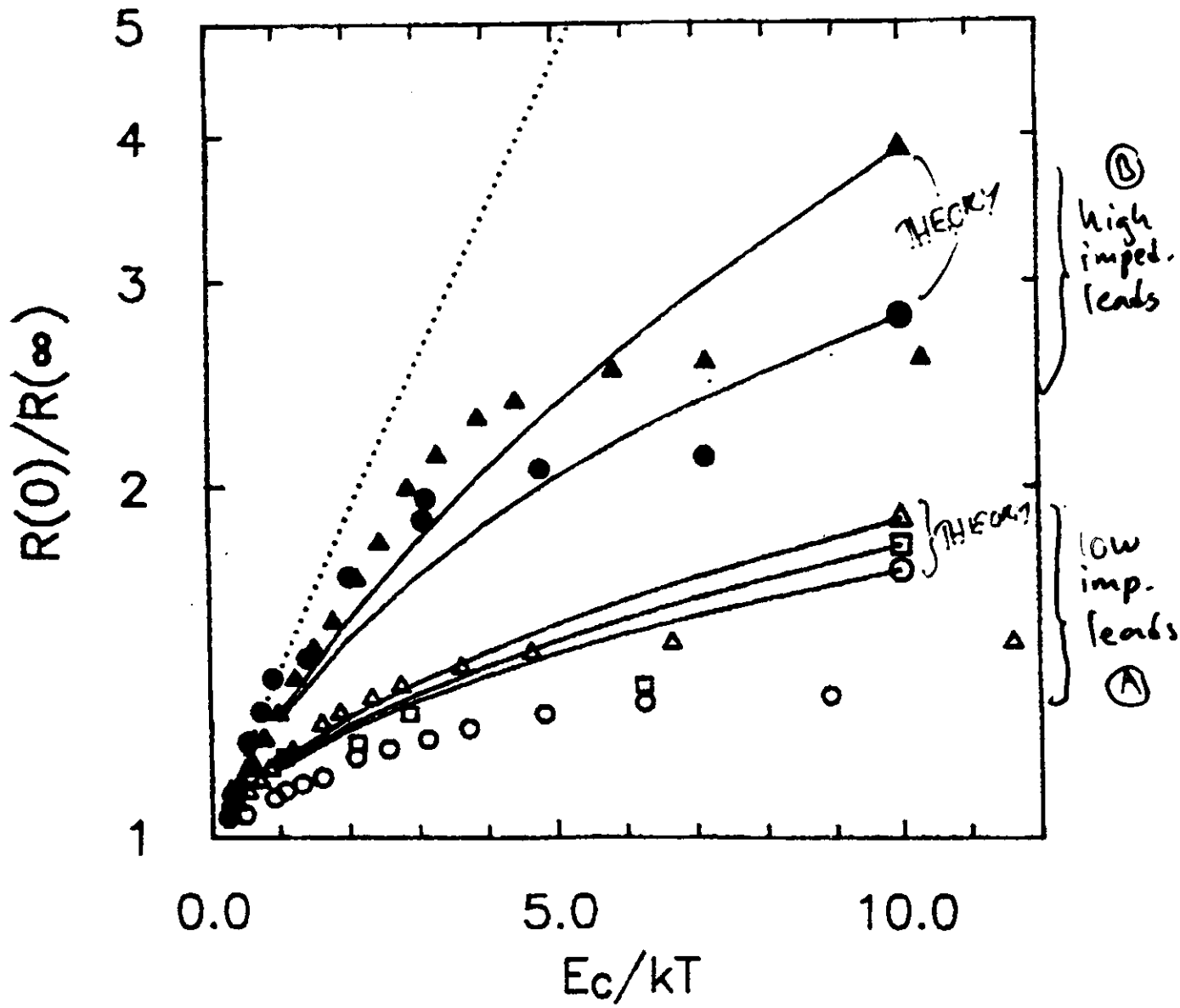

Question: Can we go beyond perturbation theory in "R_n/R_o" and (within our model) include quantum charge fluctuations across the junction?

Answer: Maybe. Map to problem of classical, interacting charges.

Recall the model Hamiltonian we used

$$H = \underbrace{\sum_k \epsilon_k c_k^+ c_k + \sum_p \epsilon_p d_p^+ d_p}_{H_{0,e}} + \underbrace{\sum_\alpha \hbar\omega_\alpha (q_{+\alpha}^+ q_{+\alpha} + 1/2)}_{H_{0,B}}$$

$$+ \underbrace{\frac{(Q+q_o)^2}{2C_0}}_{\text{coupling term}} + \underbrace{T \sum_{kp} (c_k^+ d_p + \text{c.c.})}_{\text{tunnel Hamiltonian}}$$

$$Q = \frac{e}{2}\left(\sum_p d_p^+ d_p - \sum_k c_k^+ c_k\right)$$

A canonical transformation replaces the coupling term by a new tunnel Hamiltonian

$$H = H_{0,e} + H_{0,B} + V \; ; \quad V = T \sum_{kp} (c_k^+ d_p \underbrace{e^{i\varphi_0}}_{\text{displacement operator on Lm junction, charge: } q \to q+e} + \text{c.c.})$$

Next step is to find the partition function Z.

$$Z = \mathrm{Tr}_B \mathrm{Tr}_e \left\{ e^{-\beta H_{0,B} - \beta H_{0,e} - \int_0^\beta d\tau\, V(\tau)} \right\}$$

Use ideas in Ambegaokar, Eckern & Schön PRL 48, 1745 ('82) to trace out (approximately) the electronic degrees of freedom

$$Z \simeq \mathrm{Tr}_B e^{-\beta H_{0,B}} \exp\left\{ \frac{1}{2} \int_0^\beta d\tau \int_0^\beta d\tau' \langle T_\tau V(\tau) V(\tau') \rangle \right\}$$

↑ electron system assumed to return to equilibr. after tunneling events. Interactions via collective modes

$$\langle T_\tau V(\tau) V(0) \rangle = \alpha_T(\tau) \left\{ e^{-i p_0(\tau)} e^{i p_0(0)} + \text{c.c.} \right\}$$

$$\alpha_T(\tau) = \frac{1}{4\pi^2} \frac{R_H}{R_0} \frac{(\pi/\beta)^2}{\sin^2(\pi\tau/\beta)} \sim \frac{1}{\tau^2}$$

We shall need to trace out the collective ("boson") degrees of freedom. This can here be done exactly (harmonic oscillators)

The resulting Z describes a system of classical, interacting particles :

Equivalent Classical Stat. Mech. Problem:

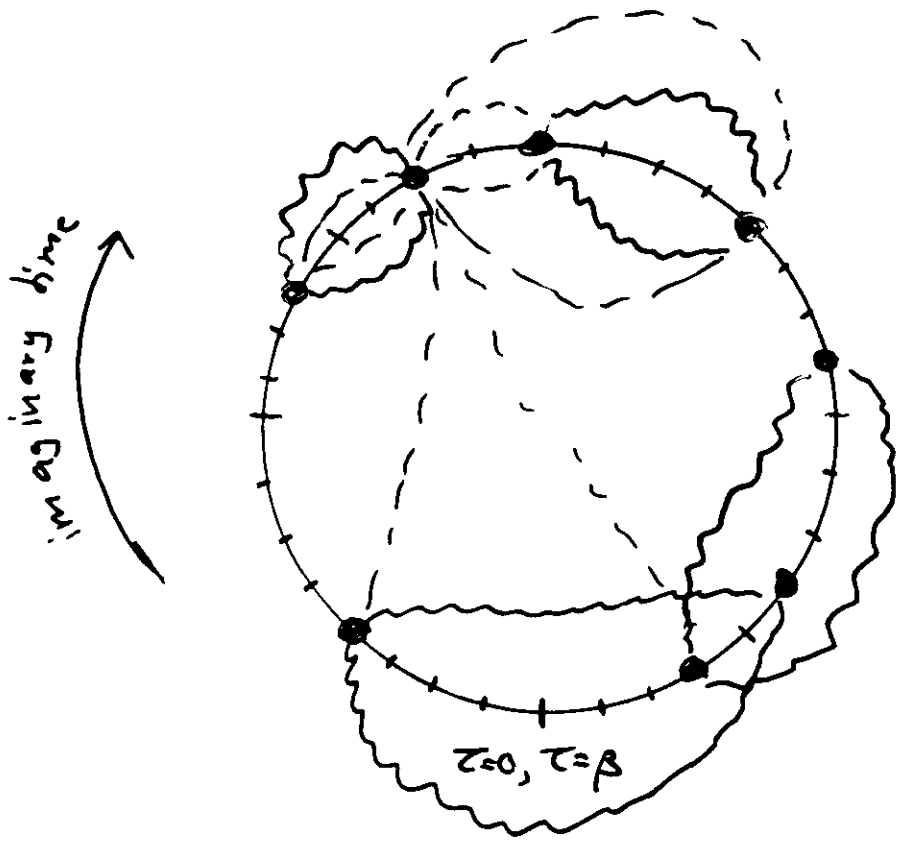

$$Z = \sum_n \frac{1}{n!} \sum_{\{\sigma_j\}} e^{\sigma_k \Lambda_{kj} \sigma_j}$$

$$\sigma_k = \begin{cases} +1 & (\text{jump} \rightarrow) \\ -1 & (\text{jump} \leftarrow) \end{cases}$$

$$\Lambda_{kj} = \underbrace{-\ln \alpha_{kj}}_{\text{interaction between "pairs" of "charges"}} + \underbrace{\frac{1}{2} G_{kj}}_{\text{interaction between all "charges" due to e-m environment.}}$$

$$\approx \ln \tau_{kj}$$

" ~~~~ "

$$G_{kj} = -\frac{e^2}{\hbar} \langle T_\tau P_0(\tau_j) P_0(\tau_k) \rangle$$

$$\sim \begin{cases} \epsilon_c |\tau_{jk}| & \tau_{jk} \to 0 \\ \frac{2Z(0)}{R_H} \ln |\tau_{jk}| & |\tau_{jk}| \text{ large} \end{cases}$$

" - - - - - - "

Screening effects from "---" can affect time ordering of charges (jumps) and hence the conductivity

Some evidence for phase transition from a Coulomb blockade state to a coherent conducting state was found in earlier work

See for instance Scalia et al Z. Phys. B 85, 427 ('91) [1]
Zwerger and Scharpf, -"-, 421 ('91) [2]

who work in the "phase"-representation rather than the "charge" representation outlined above.

In their model "g" is not varied, coupling to environment gives in a sense classical Coulomb blockade "$A(\omega) \sim \delta(\omega - E_c)$".

1) Monte-Carlo study

2) Analytical work
Panyukov and Zaikin, PRL, 3168 (1991)
Predict phase transition as function of "g".

Some trivial limits of conductivity calculated in linear response from Kubo formula:

(i) $g \equiv \frac{2\mathcal{E}(0)}{R_H} = 0 \Rightarrow$ ohmic result $R(i\omega) = R_0$

(ii) $g \neq 0$, $R_H/R_0 \to 0$, recover result of TL (perturbation) theory $R(i\omega) \sim (i\omega)^{-g}$

Looking for interesting, non-trivial behaviour as function of

g (coupling to environment)

α_T (nominal junction resistance)

β (temperature)

But no firm results yet

Time correlated tunneling. A new standard for current??

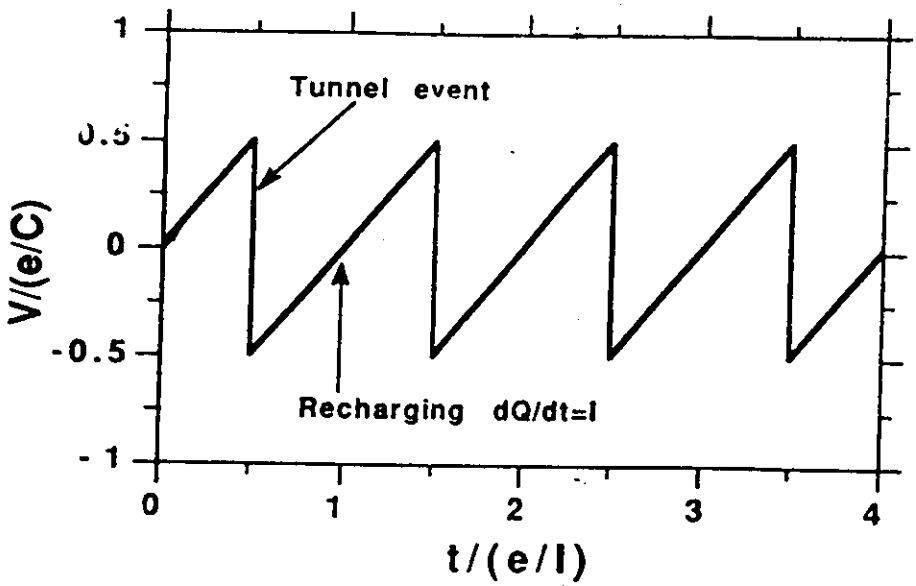

Fig.2.4 The SET-oscillations in a current biased SET junction at low currents (I<<e/RC).

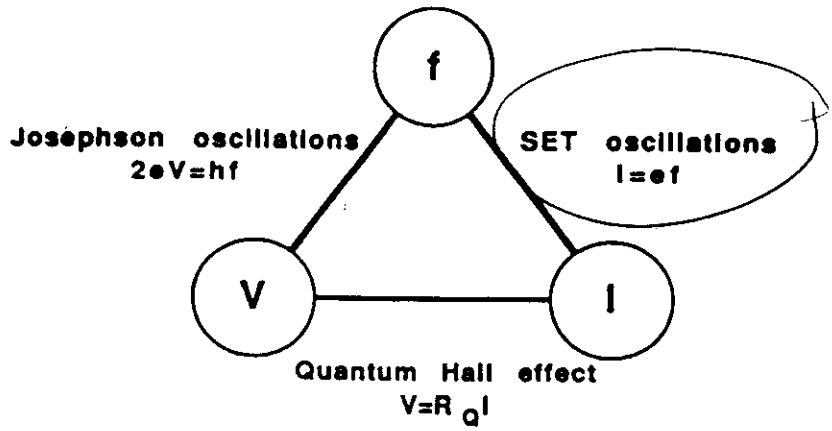

$I = ef$

Fig.2.5 The Quantum Triangle.

Tunneling throug microwave irradiation

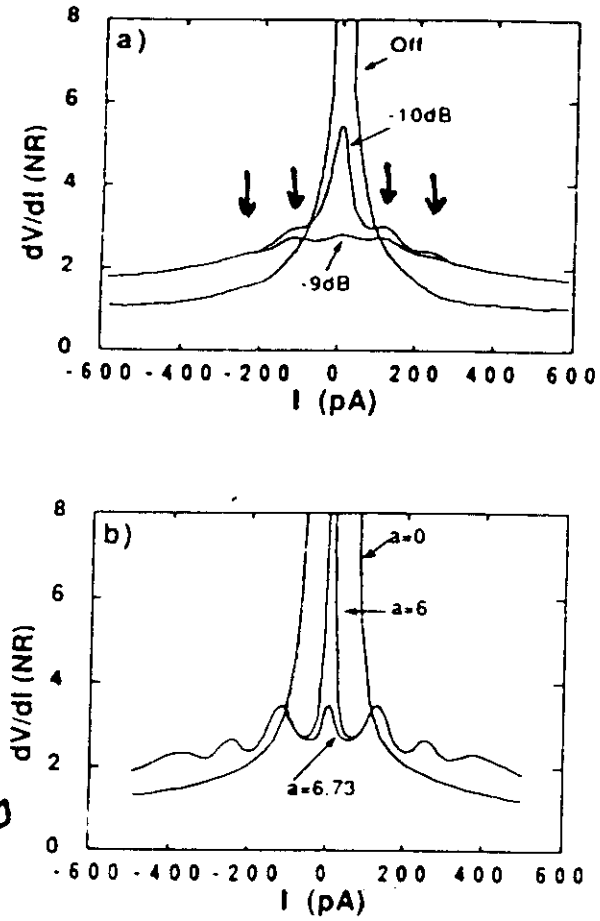

exp.

theory

Delsing et al., Phys. Rev. Lett. 63, 1861 (1989)

Fig.9. The differential resistance (R_d = dV/dI, normalized to the array resistance) of array 2.2 as a function of bias current and at different microwave radiation powers. (a) Experimental curves for no radiation power and for relative dampings of -10 and -9 dB. T= 50 mK. f=0.75 GHz. The ac modulation of the derivative measurement was about 5 pA rms. (b) Corresponding theoretical curves with relative microwave amplitudes of a=0, 6, and 6.73, where a is the normalized voltage amplitude ($a=A_{m.w}/(e/C)$) of the microwaves. The parameters used were the same ones as for the calculations for Fig.6b.

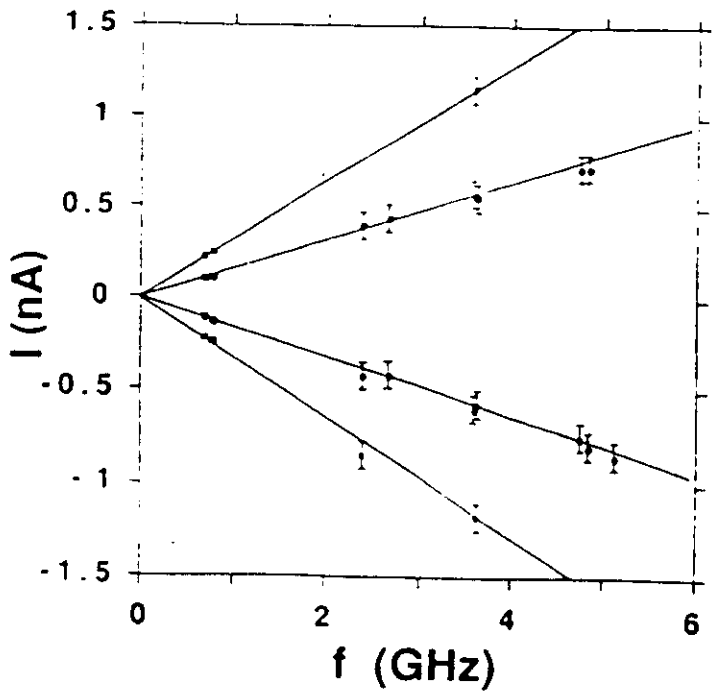

$I = nef$

$n = \pm 1, \pm 2$

Fig.10. The locations of the differential resistance peaks (and shoulders) at applied radiation as function of microwave frequency. Data are given for arrays 1.5 (N=23) 2.1 (N=15) and 2.2 (N=19). The lines are given by I=nef with n=±1, ±2.

Frequency-locked tur[illegible] device for single electrons.

L.J. Geerligs, V.F. [illegible]eregg, P.A.M. Holweg,[a] J.E. Mooij
Department of Applied Physics, Delft University of Technology,
P.O. Box 5046, 2600 GA Delft, The Netherlands

H. Pothier, D. Esteve, C. Urbina, M.H. Devoret
Service de Physique du Solide et de Résonance Magnétique,
Centre d'Études Nucléaires de Saclay, 91191 Gif-Sur-Yvette, France

ELECTRON "TURNSTILE"

Figure 1.
Principle of controlled single electron transfer through a linear array of small tunnel junctions. Junctions, with capacitance C, are denoted by crossed capacitor symbols, the gate voltage V_g is applied via a true (non-tunneling) capacitance C_g. If C_g=C/2, tunneling across any junction can only occur if for that junction |Q|>Q_c, with Q_c=e/2. The voltages and charges are indicated in units of e/C and e. 1-6 indicate consecutive times in the cycle. Left: First half of the cycle, V_g=2. An elementary charge (- in a circle) ends up trapped on the central electrode. Right: Second half of the cycle, V_g=0. The charge can only leave on the right hand side. No further tunneling can occur in the emptied array.

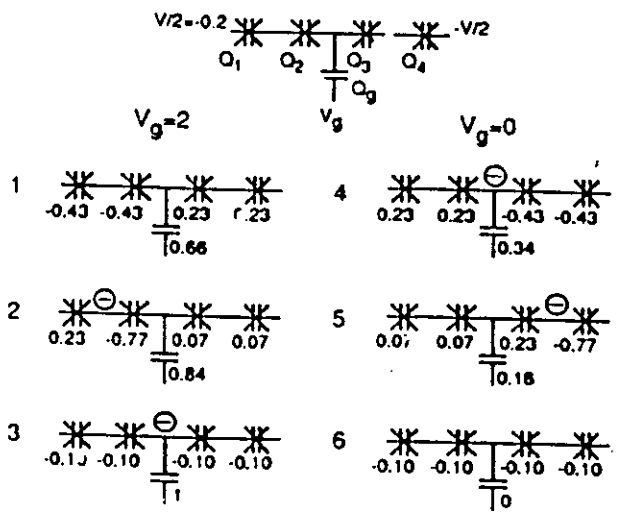

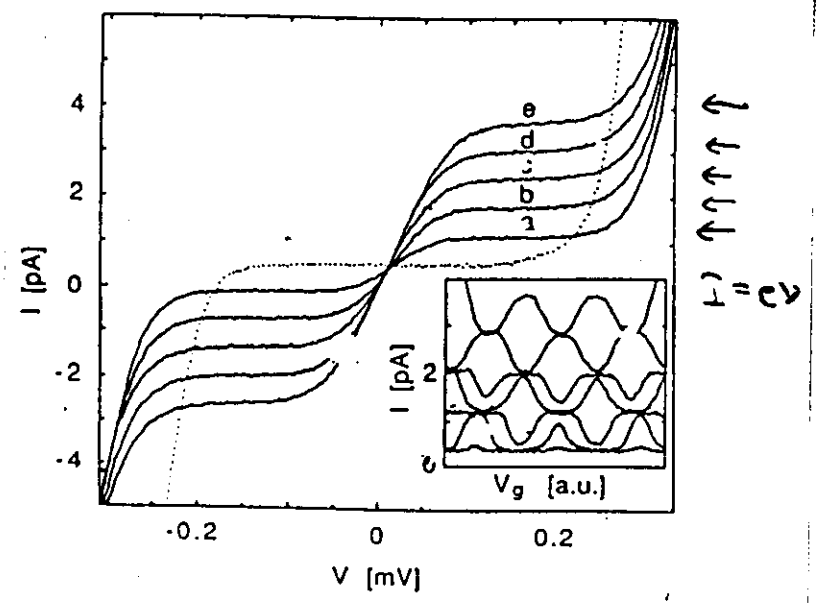

Figure 2.
Current-voltage characteristics without ac gate voltage (dotted) and with applied gate voltage at frequencies f from 4 to 20 Mhz in 4 Mhz steps (a-e). Current plateaus are seen at I=ef. The inset shows current versus dc gate voltage characteristics for f=5 MHz. The curves tend to be confined between levels at I=nef and I=(n+1)ef, with n integer. The bias voltage was fixed at 0.15 mV. For the bottom curve, which is nearly flat, the ac gate voltage amplitude is 0. For the other curves the calculated ac amplitude at the sample increases from 0.60e/C for the lowest one to 3.4e/C for the upper one, where e/C=0.30 mV.

THE ELECTRON "PUMP"

Pothier et al. Physica B 169, 573 (1991)
Geerligs et al. Z. Phys. B 349 (1991)

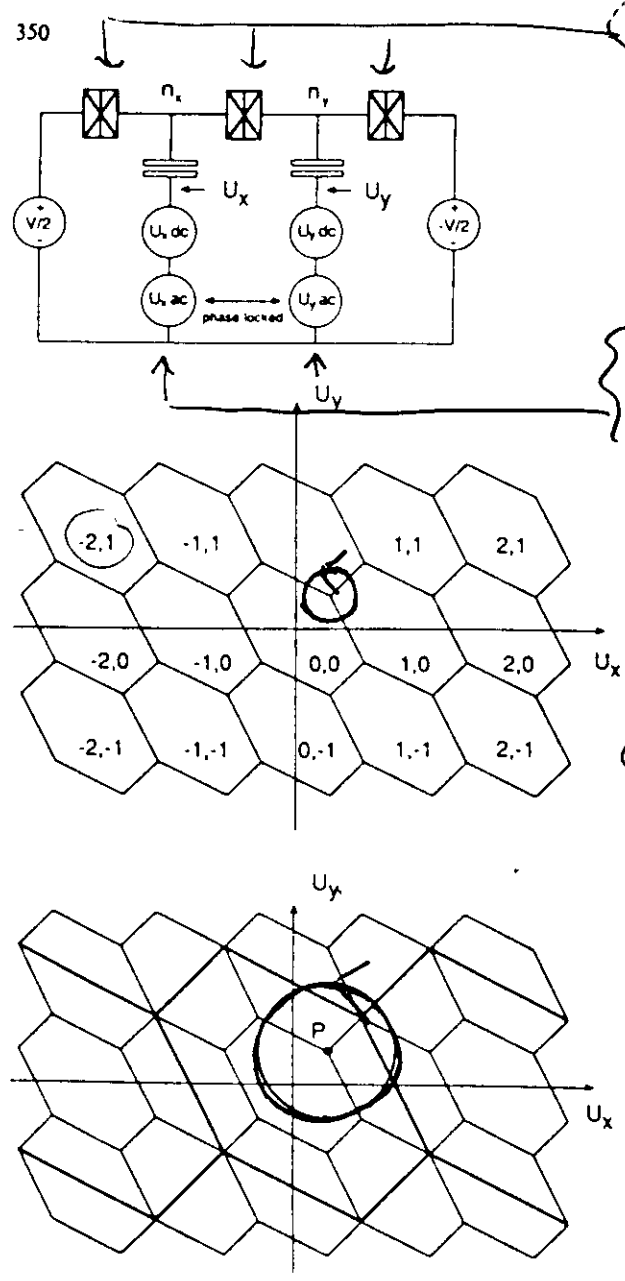

TUNNEL JUNCTIONS

FIX PHASE DIFFER. BETWEEN DRIVING AC-VOLTAGES U_x, U_y

(n_x, n_y)

DIAGRAM SHOWING EQUILIBRIUM CONFIG OF (n_x, n_y)

(THICK LINE FOR SUPER-CONDUCTING STATE)

Fig. 1. a Schematic picture of the single Cooper pair pump. The crossed boxes denote the tunnel junctions. Two alternating gate voltages will move charges (quasi-)adiabatically one by one through the tunnel junctions. b The lowest energy charge configuration as a function of the gate voltages U_x and U_y. Following the circle one electron is transferred through the device. c The lowest energy charge configuration in the superconducting state. The thick lines give the cell boundaries in the superconducting state. The thin lines give the cell boundaries where a quasiparticle can tunnel

I-V of microwave irradiated electron "pump"

(normal state)

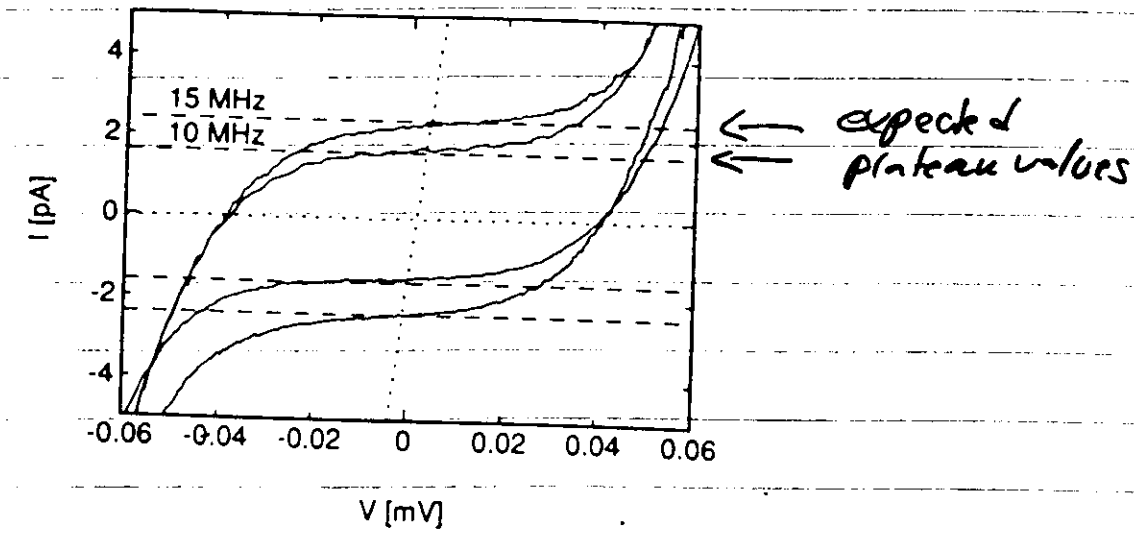

Fig. 3. Current-voltage characteristics at 10 and 15 MHz in the normal state. The dotted curve is the $I-V$ curve without rf applied, the horizontal one with the gate voltage adjusted in the middle of a cell (maximal Coulomb gap) and the other with the gates adjusted at a triple point (minimal Coulomb gap). The positive and negative plateaus are obtained by choosing the appropriate phase difference. The dashed lines are at the expected values of $I = ef$. $T < 50$ mK

direction (sign) of current depends on choise of phase difference between driving ac-voltages.

To minimize "leakage" currents

Use arrays.

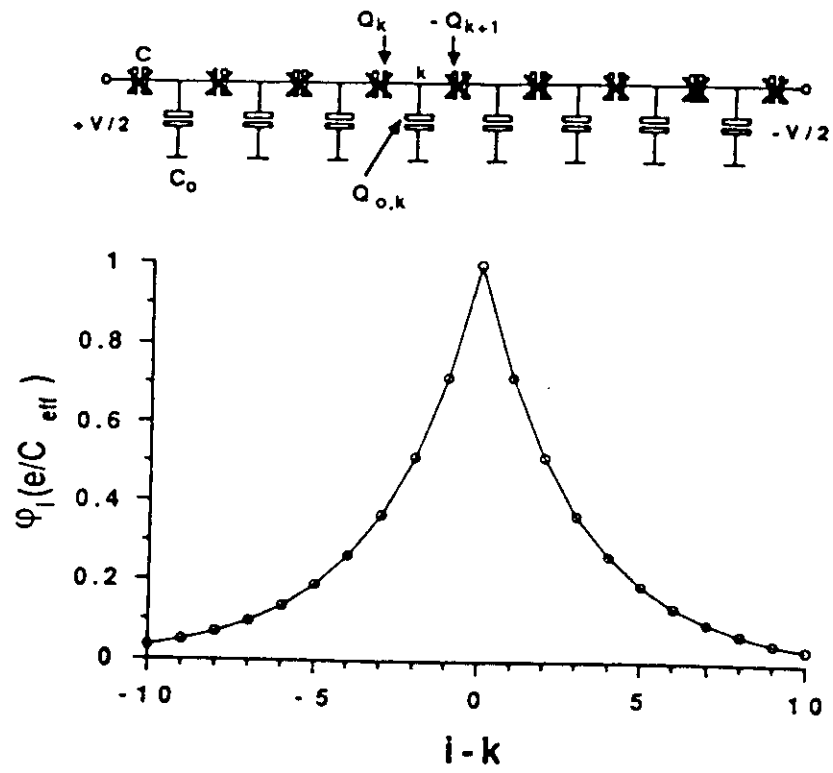

charge "solitons" move through array.

A charge, e, on one junction, that is a member of a long array of series coupled junctions, affects the charge distributions on surrounding junctions. A charge soliton is formed. Its charge equals the supplied charge, e, and its extension is given by the junction and stray capacitances. It typically is of the order of a few junctions for common array parameters. The upper part of the figure shows an array of junctions, each of which has a capacitance of C and with stray capacitance C_o to ground from each intermediate electrode. The charge distribution on electrode k is shown. The lower part of the figure shows the potential distribution on the electrodes around the charged electrode k of a long homogeneous array with M=3.

25 junction array turnstile

Delsing et al. PRL 63, 181 (1989)

ibid

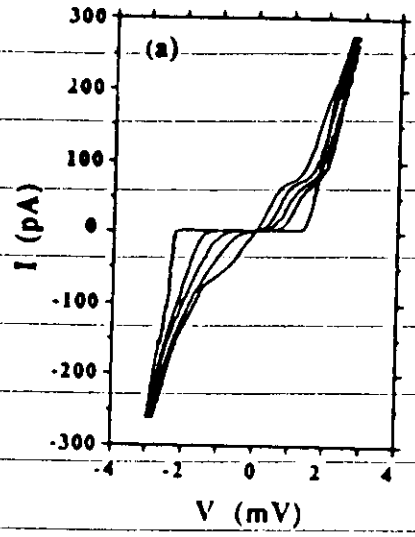

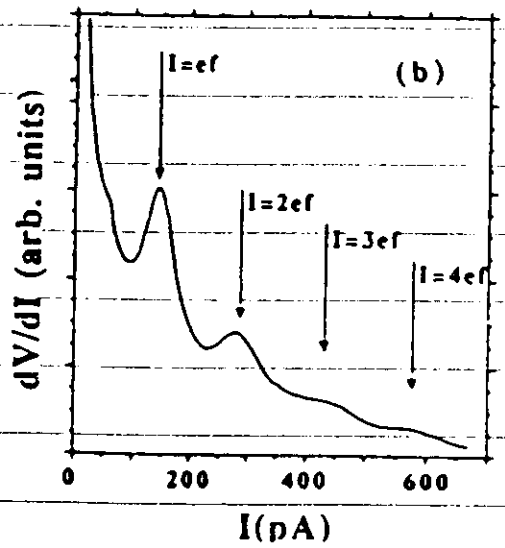

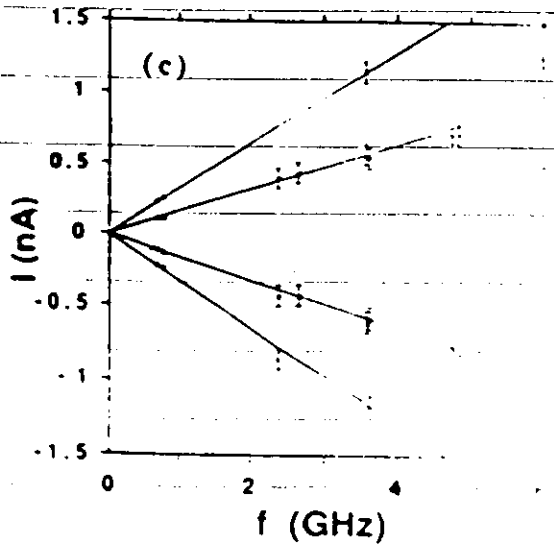

Figure 3. (*a*) *I–V* curves for a 25 Al junction array with increasing power of microwaves (435 MHz). $R \approx 60$ kΩ, $C \approx 0.3$ fF per junction, $T \approx 35$ mK. A magnetic field of 0.3 T was applied. (*b*) Differential resistance as a function of current for a 25-junction array with microwaves applied at a frequency $f = 0.9$ GHz. The peaks fall close to their expected values, $I = nef$. Note that there is even a sign of a subharmonic peak at about 70 pA. Superconductivity was quenched by a magnetic field. $T = 50$ mK. (*c*) Frequency dependence of the DC current positions of the $n = \pm 1$ and $n = \pm 2$ resistance peaks for three arrays with $N = 12$, 15, and 19. The lines have slopes $\pm e$ and $\pm 2e$. The data points fall close to these lines in good accord with the theory of time-correlated tunnelling. From [4, 5].

Single Electron Tunneling – Transistors

for

1) Electrometers

2) Signal amplification

Capacitive coupling

Resistive coupling

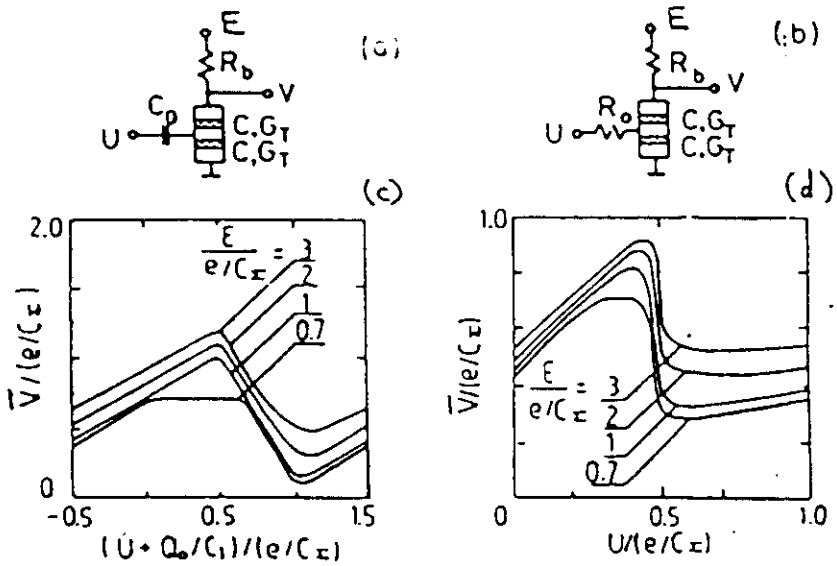

(calculated)

Fig. 39

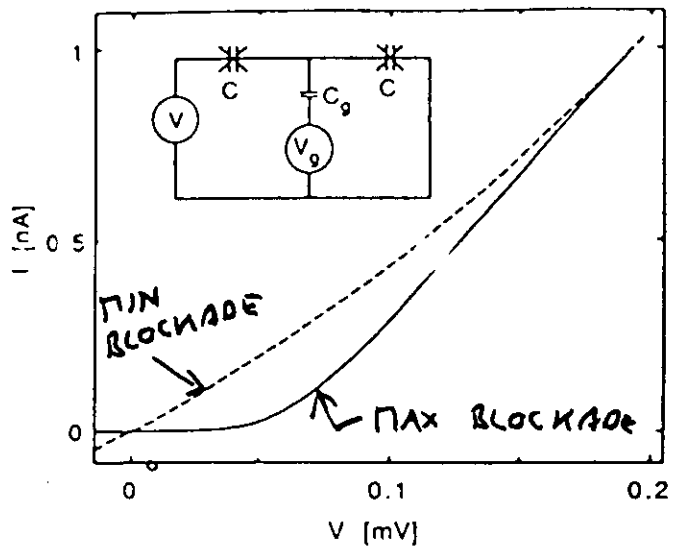

T = 10mK

Geerligs et al.
PRL 65, 377 (1990)

{GATE VOLTAGE V_G AFFECTS COULOMB BLOCKADE}

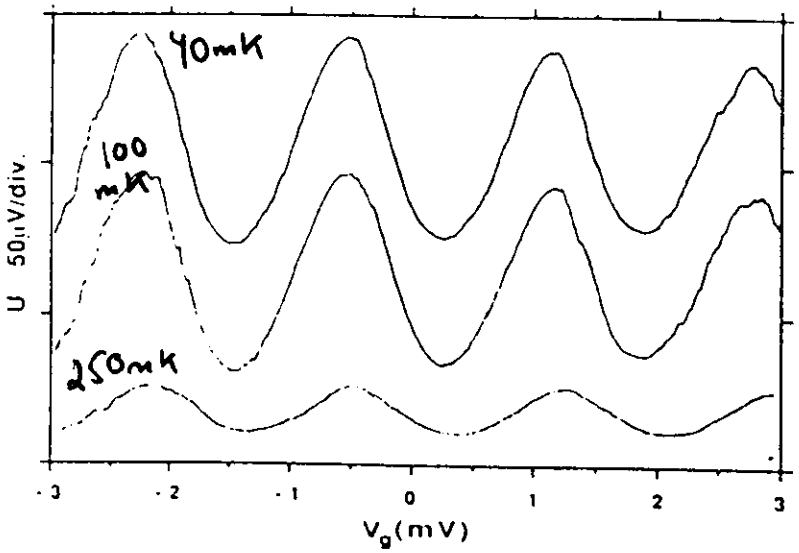

ELECTROMETER
(MEAS. CHARGE)

Kuzmin et al.
PRL 62, 2539 (1989)

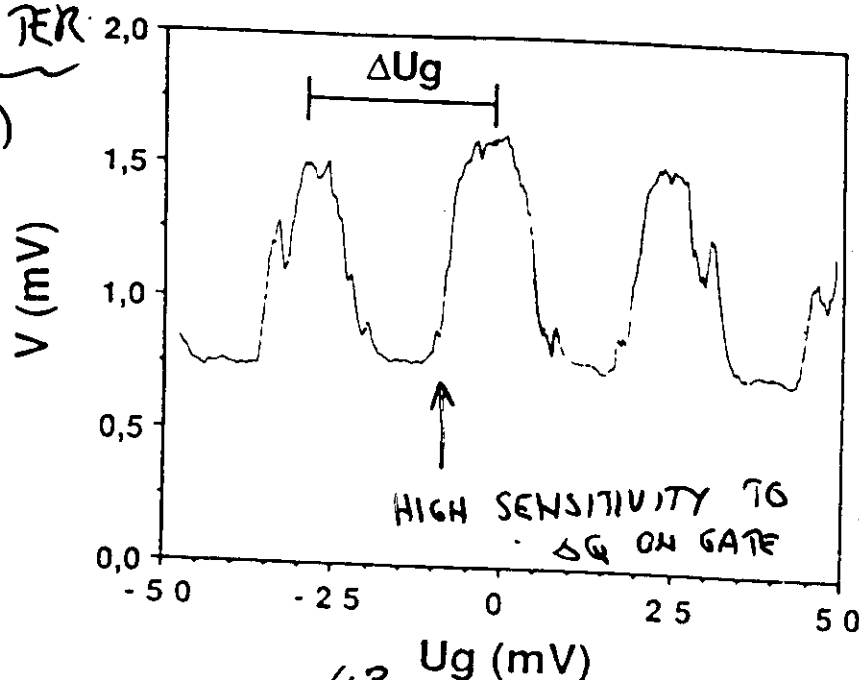

T = 1.3K
13 junction array

$\simeq 10^{-4}$ e

SET - transistors (c-2)

for

c) digital integrated circuit

Estimates of the main parameters of the single-electron tunnel junctions (after Likharev 1987a,b)

Levels of the fabrication technology	Junction area S (nm^2)	Junction capacitance C (10^{-18} F)	Temperature limit T_{max} (K)	Voltage scale $V_t = e/2C$ (mV)	Power scale $P = V_t^2 C_T$ [b] (W)	Time scale $\tau = C/C_T$ (ps)	Active device density n ($gates/cm^2$)
State-of-the-art junctions	30x30	30	30	2.5	10^{-11}	3	$\sim 10^9$
Apparent limits of the nanolitography	10x10	3	300	25	10^{-9}	0.3	$\sim 10^{10}$
Hypothetic macromolecular structures	3x3	0.3	3000	250	10^{-7}	0.03 [c]	$\sim 10^{11}$

a) Defined as $10^{-2}(e^2/2C)$.

b) C_T^{-1} is accepted to equal 600 kOhm ($\alpha_T \sim 10^{-2}$).

c) Some other (larger) time scale may be more relevant for the size so small, see section 6.5.

From Likharev's review

Bloch oscillations

(Likharev, LTP 17 (1984) and J. Low Temp Phys later)

Recall: $I = I_c \sin\varphi$ $\qquad I \propto \frac{dE}{d\varphi}$

$\downarrow$

$E \propto -I_c \cos\varphi \Rightarrow \boxed{E = -E_J \cos\varphi}$

But the total energy (and Hamiltonian) will depend on other things also

$$\mathcal{H} = \underbrace{\frac{Q^2}{2C}}_{\text{energy of the "capacitor"}} \underbrace{- E_J \cos\varphi}_{\text{Josephson coupling}} + \text{other terms}$$

important if C is small

$$\text{Q.M.} \quad [Q, \varphi] = \underbrace{2ei}_{\neq 0}$$

$= 2e\mathcal{H}$ ↑ phase
↳ amplitude

Compare electron : $[p, x] = i\hbar$

there we choose $p = -i\hbar \frac{\partial}{\partial x}$

Here take $Q = -i2e \frac{\partial}{\partial \varphi}$

$$\mathcal{H} = -E_Q \frac{\partial^2}{\partial \varphi^2} - E_J \cos\varphi + \dots$$

Compare electrons in a periodic lattice which can (in principle) have Bloch oscillations

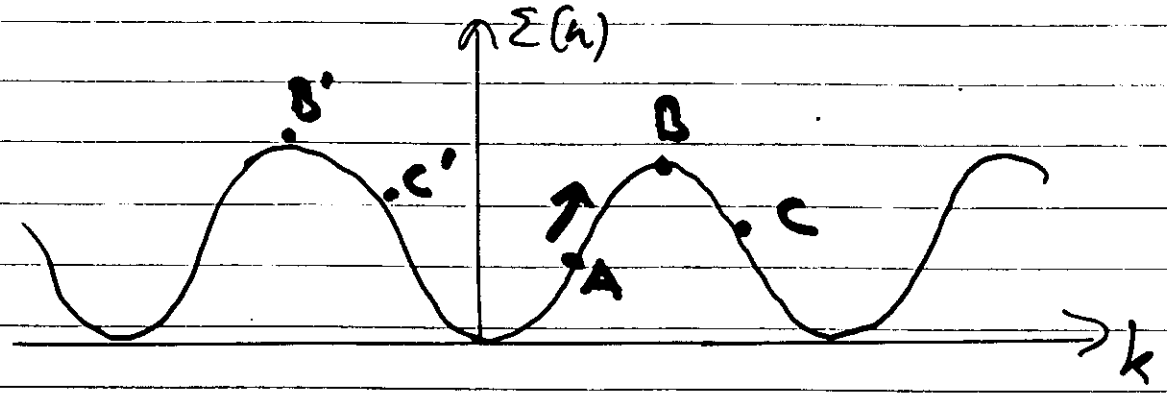

$v_k \propto \frac{\partial E(k)}{\partial k}$ $\quad k(t) \propto eEt$

v_k and I periodic in time (if no scattering)

(Bloch oscillations)

SUPERCONDUCTING JUNCTIONS

ADD PARAMETER E_J (JOSEPHSON COUPLING ENERGY)

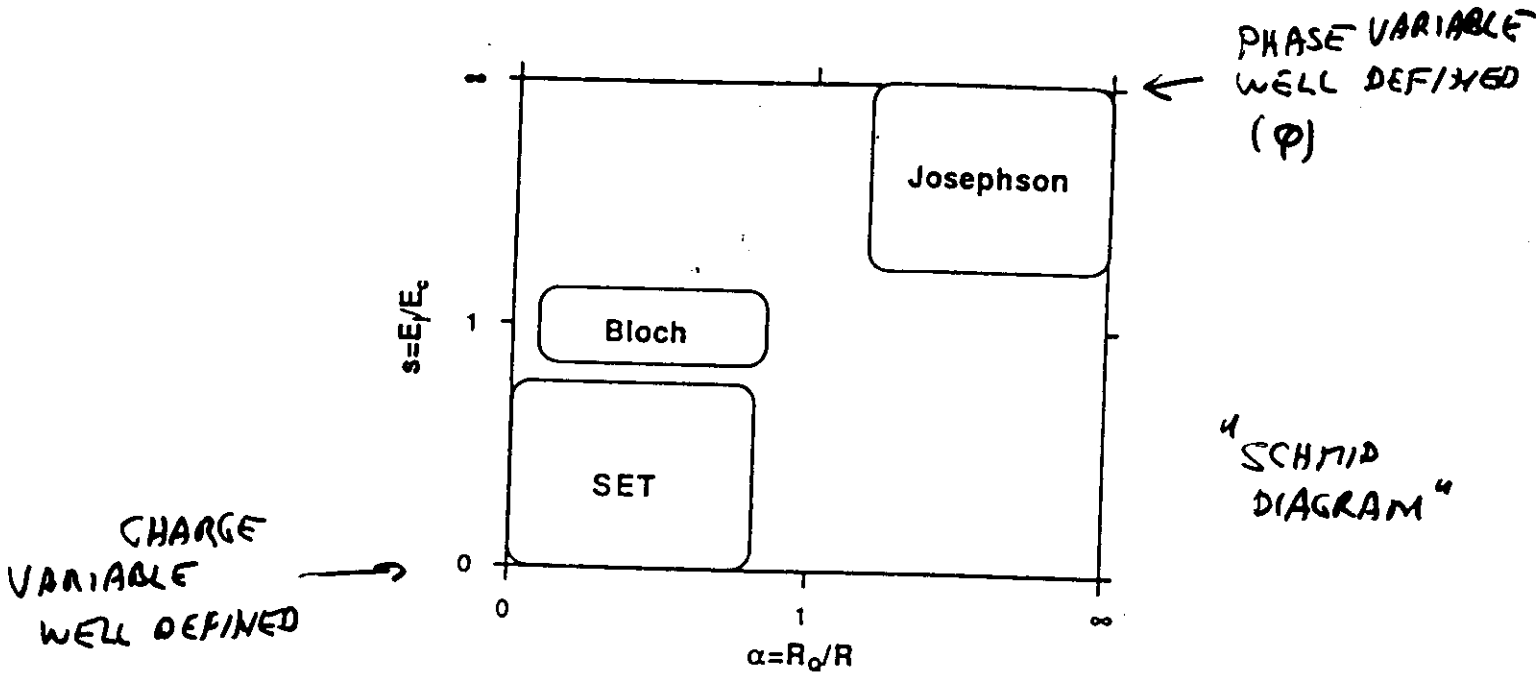

Fig 1.2 Phase diagram showing different limits for a tunnel junction.

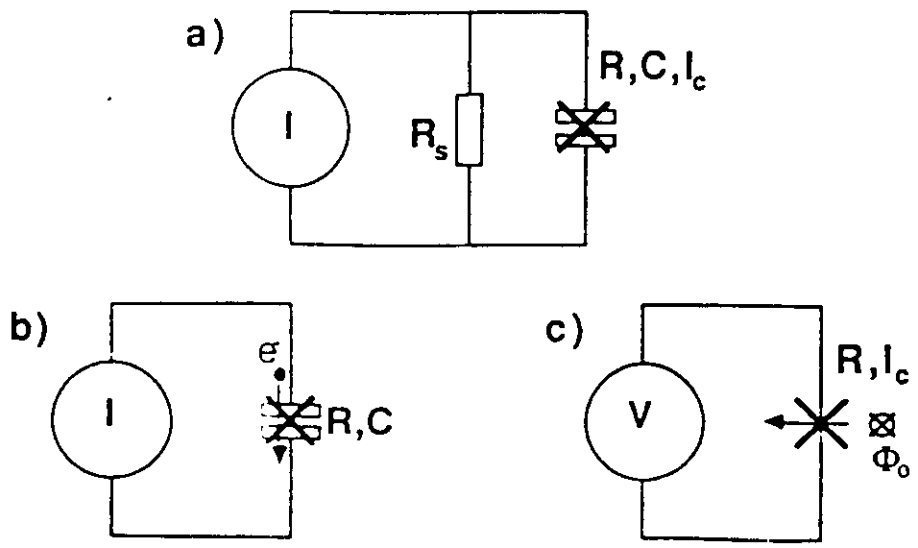

Fig.1.3 a) The general circuit b) The SET limit : a current biased junction where single electrons tunnel across the barrier c) The Josephson limit : a voltage biased junction where single flux quanta are transfered across the junction.

BLOCH-OSCILLATIONS IN S.C. JUNCTIONS

Haviland et al. Z. Phys. B 85, 339 (1991)

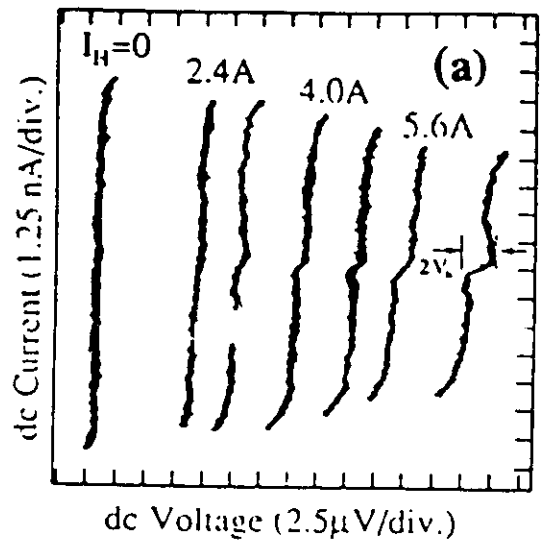

increasing B-field
decreasing E_J
increasing Coulomb blockade

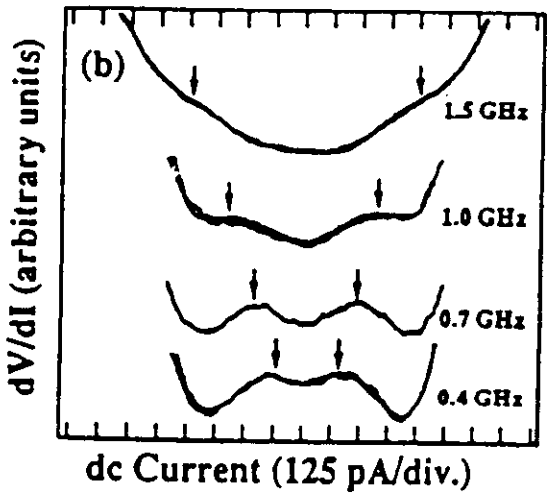

irradiated S.C. junction
peaks in dV/dI
(≈ current plateaus)

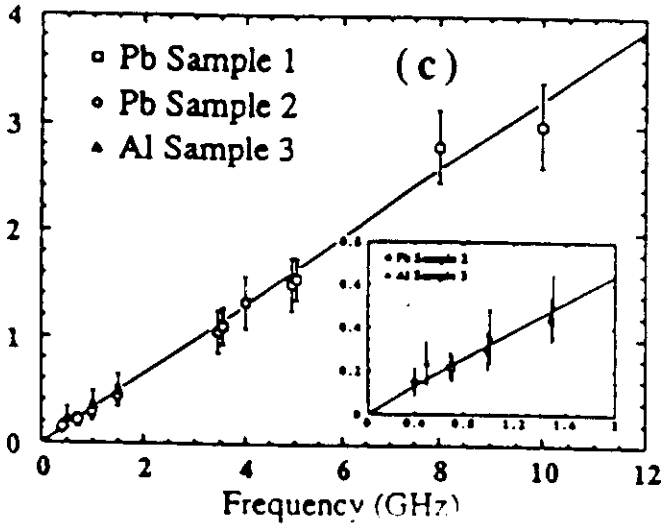

peak position
vs. frequency

6. (*a*) The effect of magnetic field on the *I–V* curve of a Pb alloy junction, $R_N \approx 8.5$ kΩ, $R_{load} \approx 95$ kΩ, $E_J \approx 400$ μeV, $E_C \approx 200$–300 μeV (depending upon method of evaluation), $T = 60$ mK. $I_H = 1$ A corresponds to a magnetic field of about 0.3 kG at the junction. (*b*) The dynamic resistance as a function of DC current for a Pb alloy sample with $R_N \approx 56$ kΩ, $R_{load} \approx 95$ kΩ, $E_J \approx 60$ μeV, $E_C \approx 200$–600 μeV, $T = 60$ mK at four microwave frequencies. Two traces of each curve indicate the noise level. The arrows mark $I = \pm 2ef$. (*c*) The half-distance in current between peaks in dV/dI as a function of f. Sample 1 is the junction of (*a*), sample 2 of (*b*), sample 3 an Al junction similar to the one in figure 5(*a*) but with $R_N \approx 3.2$ kΩ, $R_{load} \approx 200$ kΩ, $E_J \approx 200$ μeV, $E_C \approx 80$–180 μeV.

Coulomb Blockade of Cooper pair tunneling

Haviland et al. Europhys Lett. 16, 103 (1991)

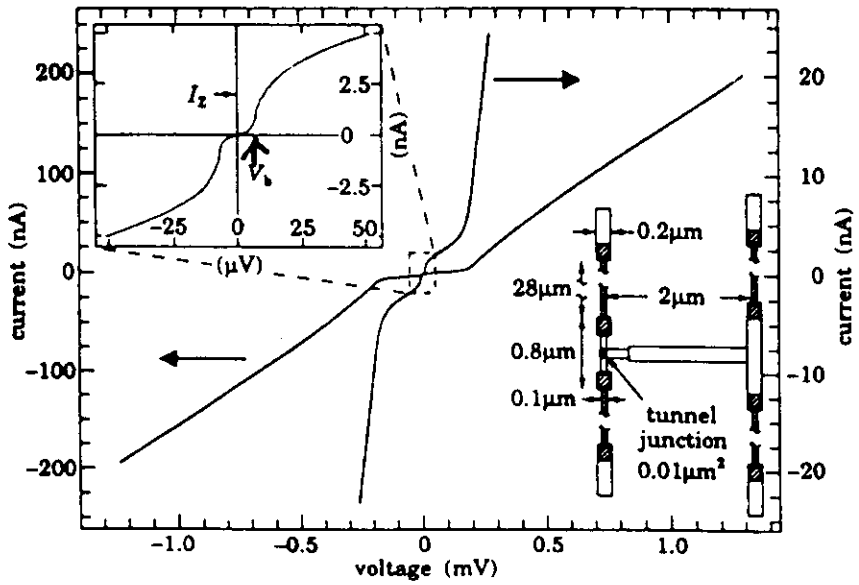

Fig. 1. – The I-V curve for sample 1 (T = 50 mK). A magnification of the current by 10 times is shown. The upper left inset is a blow-up of the central region showing the blockade voltage V_b, which is due to the Coulomb blockade of Cooper pair tunnelling. Also shown is the theoretical value of the Zener current I_Z. The lower right inset shows a schematic of the four-point measurement scheme used: □ electrodes, ■ resistors.

A → L larger B-field
⇒ smaller E_J ⇒ larger blockade

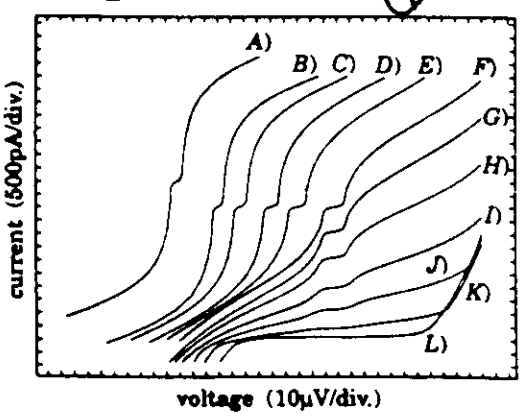

Fig. 2.

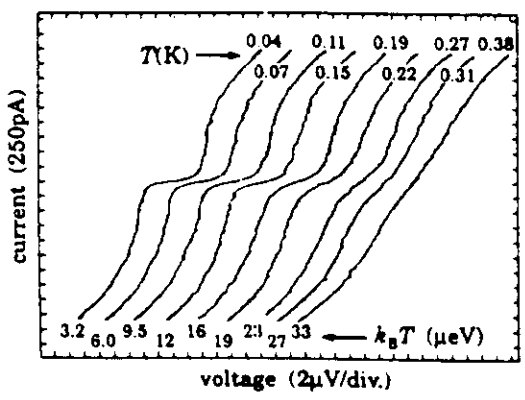

Fig. 3.

Blockade is washed out by temperature

Fig. 2. – The effect of suppressing E_J with a magnetic field is shown for sample 3 (T = 42 mK). The I-V traces are expansions of the central region as in fig. 1. Curve A) is taken in zero magnetic field, whereas in curves B) to L) the magnetic field is increased from approximately H = 160 G to 600 G. The origin is displaced for each curve for clarity.

Fig. 3. – The temperature dependence of the blockade voltage is shown for sample 3, in zero magnetic field (curve A) of fig. 2). The temperature values are listed above each curve, and the corresponding energy, $k_B T$, is listed below each curve.

cont'd

For very small E_J/E_C

mostly Cooper pair tunneling

A → E
higher B
smaller E_J
less pair-tunneling

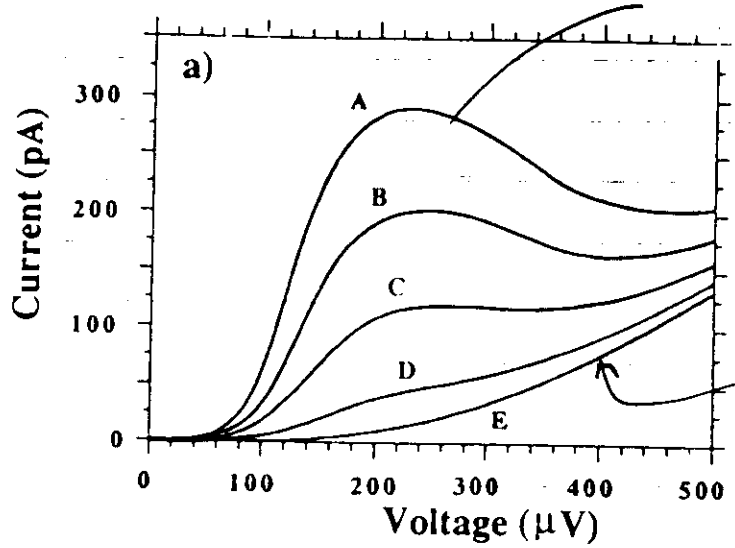

only quasi-particle tunneling

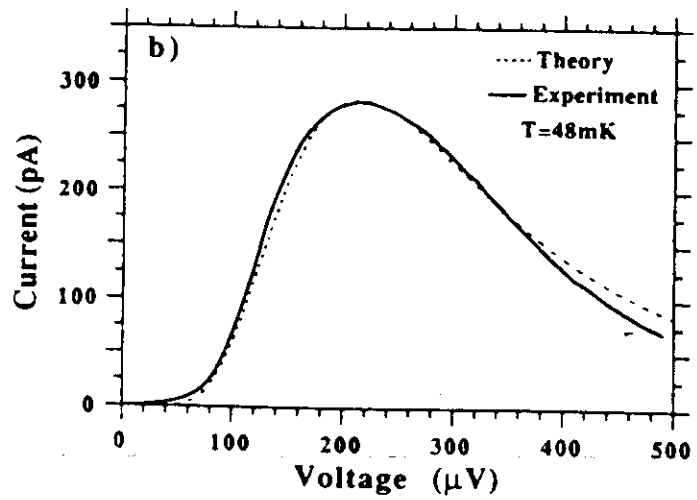

q.p. tunneling subtracted off

I_{pair} ∝ "A(ω)"

Fig. 4. **a** The experimental I–V curves of a Pb-alloy Josephson junction (sample 10) in different magnetic fields. From curves A to E the magnetic field values are $H = 0$ G, 480 G, 720 G, 1.1 kG and 1.6 kG respectively. **b** The experimental, $H = 0$, I–V curve of the same junction, where the quasiparticle current has been subtracted off (solid line), and the fitted theoretical I–V curve (dashed line)

SET limit

$q \longleftrightarrow \Phi$

$e \longleftrightarrow \Phi_0 = h/2e$

$E_c = \frac{e^2}{2C} \longleftrightarrow E_J$

$I \longleftrightarrow V$

etc.

JOSEPHSON limit

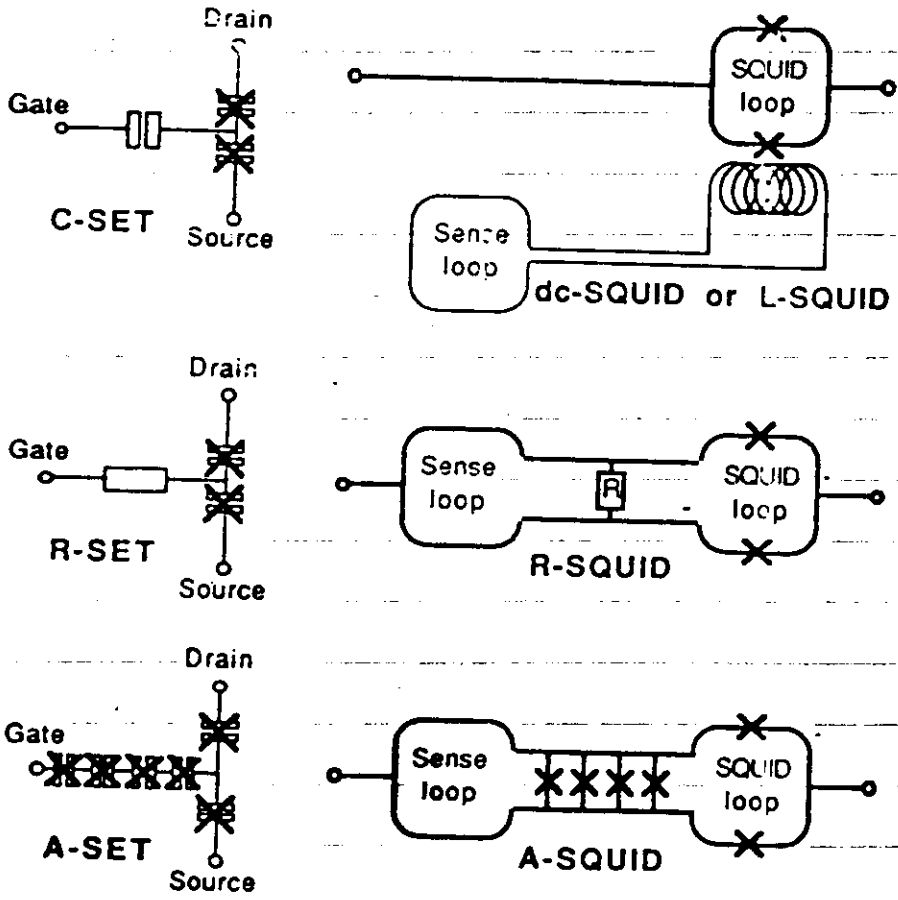

Fig.2.8 Three different types of SET transistors and their SQUID analogies.